Chapter 4 – Results and Discussion: RF plasma enhanced chemical vapour deposition

This chapter is divided into four sections; the first will discuss the deposition and analysis of DLC and amorphous carbon films. Analysis of these films will show which conditions within the reactor will produce the structure framework most likely to produce carbon phosphide (with reference to the theoretical work on the stable structures of carbon phosphide[1-3]). The second part of this chapter shows the effect of adding PH_3 to the gas mixture, its incorporation into amorphous films and its effect on the film properties. The third part discusses optimisation of the chamber conditions to maximise the bonding between carbon and phosphorus (by adjusting the ion energy) and again its effect on the properties of the thin film. The fourth part discusses the results of using a substrate heater *in situ* during deposition and its effect on the resulting films.

4.1 DLC and amorphous carbon thin films

Some of this work was done in collaboration with Jacob Filik, an undergraduate project student.

4.1.1 - Aims

The deposition of amorphous carbon films is a widely studied area. The study of properties of various amorphous carbon films deposited in the apparatus used in this study gives an idea of the optimum conditions for carbon phosphide growth. In this section, analysis of amorphous carbon films that have been grown at various chamber pressures and RF-powers will be presented. The XPS spectra will be studied and used as a way of assessing the sp^3 : sp^2 bonding ratio within the films.

As Lim[1], Claeyssens *et al*[2] and Shapton[4] calculated that the most favourable structure of carbon phosphide is likely to be pseudo-cubic, with carbon exhibiting sp^3 hybridisation, it follows that a good starting point in the synthesis of carbon phosphide would be to optimise conditions for the highest sp^3 bonding.

4.1.2 – Growth and Analysis Parameters

The films were grown in the RF-CVD chamber described in the experimental section (Section 3.1.1). The process gas was CP-grade methane (CH_4), supplied by BOC. The process flow rate was set at 30 standard cubic centimetres per minute (sccm). All films were grown for 30 minutes. The deposition pressures and DC-Bias voltages are shown in Table 4.1. All films in this study were grown on single crystal B doped (100) Si wafer.

The XPS spectra were taken using the Fisons Escascope described in the Experimental section. A wide scan, a close up scan of the C 1s region and a close up scan of the O 1s region were taken (the O 1s peak was taken for completeness as it was a prominent peak).

The XPS results were analysed using the software package "XPS Peak, Version 4.1". As discussed in the experimental section, the sensitivity factor affects different elements, but it does not affect different states of the same element. Therefore, if the XPS spectrum of C 1s is curve-fitted, the sp^3:sp^2 ratio of the surface of the film may be determined by directly measuring the areas underneath the fitted sp^3 and sp^2 curves. It is assumed that the surface of the film is representative of the bulk of the

film. Use of an ion source to remove the surface is not a practical idea as the ions may cause the new surface to change bonding configuration. The analysis depth of the XPS is typically around 30 Å. SRIM stopping range table calculations of C ions accelerated into a C film at energies of around 150 eV give a maximum penetration depth of 10 Å. Similar penetration is expected in this system.

Pressure /mTorr	10	20	30	40	50
DC Bias / V					
25	X		X		X
50	X		X		X
75	X		X		X
-100	X		X		X
-150	X		X		X
-200	X	X	X	X	X
-250	X		X		X
-300	X		X		

Table 4.1: Amorphous carbon films deposited in this study, cells containing X correspond to films that have been grown for this study by Jacob Filik.

The XPS C 1s curves were fitted using the method published by Leung *et al*[5]. The curves were 20% Lorentzian, 80% Gaussian, the position of the sp^3 curve was variable, the full width at half maximum (FWHM) was fixed at 1.4 eV, the sp^2 curve had its centre position linked to the sp^3 curve (the sp^2 curve had a fixed position -0.5 eV compared to that of the sp^3 curve), the FWHM was fixed at 1.3 eV. It was found that there were some inadequacies in Leung *et al*'s fitting method, as it did not take into account surface oxidation or surface contamination. It was decided to add another peak to account for this. Merel *et al*[6] identified the peak in XPS for C bonded to O in DLC films. The centre of this peak was +1.3 eV in relation to their C 1s sp^3 peak with a variable FWHM, so this peak was added.

4.1.3 Results and Discussion

The films that were produced were smooth and had a variety of colours (pink, blue, green, grey and black). Figure 4.1 shows a typical XPS spectrum taken from a DLC film produced in this study. The peak at 287 eV has been assigned to correspond to the ejection of a carbon 1s photoelectron and the peak at 535 eV has been assigned to correspond to the ejection of an oxygen 1s photoelectron. The spectra were assigned using reference [7].

The smaller peak to the right of the C 1s peak was assigned as a satellite peak produced by emission from the X-ray source by weaker lines than the Mg $Ka_{1,2}$ lines that are used to eject the electrons for the main peak. Satellite peaks are only evident in strong emission; they are always a constant energy away from any given main peak.

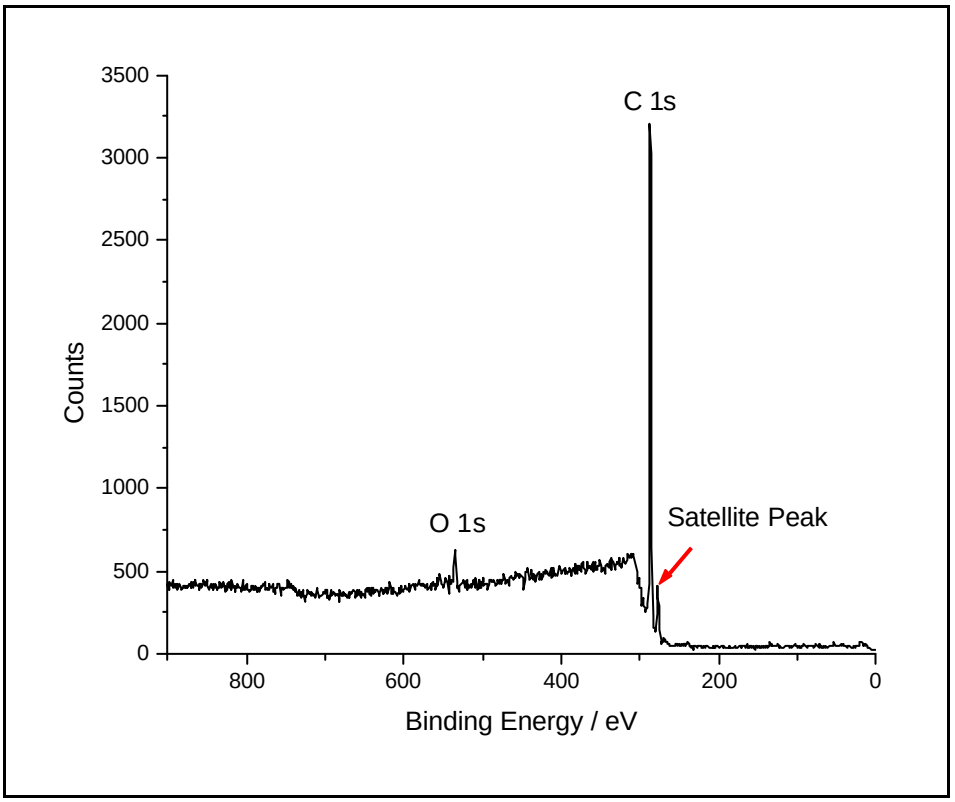

Figure 4.1: Typical XPS spectrum of DLC films produced in this study.

Figure 4.2 shows a detailed scan of the C 1s peak for a sample. It has been fitted using the two peak method suggested by Leung *et al*[5], as it can be seen at around 288 eV the peak fit fails and a large gap is left between the experimental peak and the fitted peak. In Figure 4.3 the extra peak has been added as suggested by Merel *et al*[6]. It can be seen that this allows for a much better fit. But it must be remembered that adding more curves in this case will always allow for a better fit for an asymmetric curve. Adding an extra curve is valid though if logic can be used to assign its position relative to other curves.

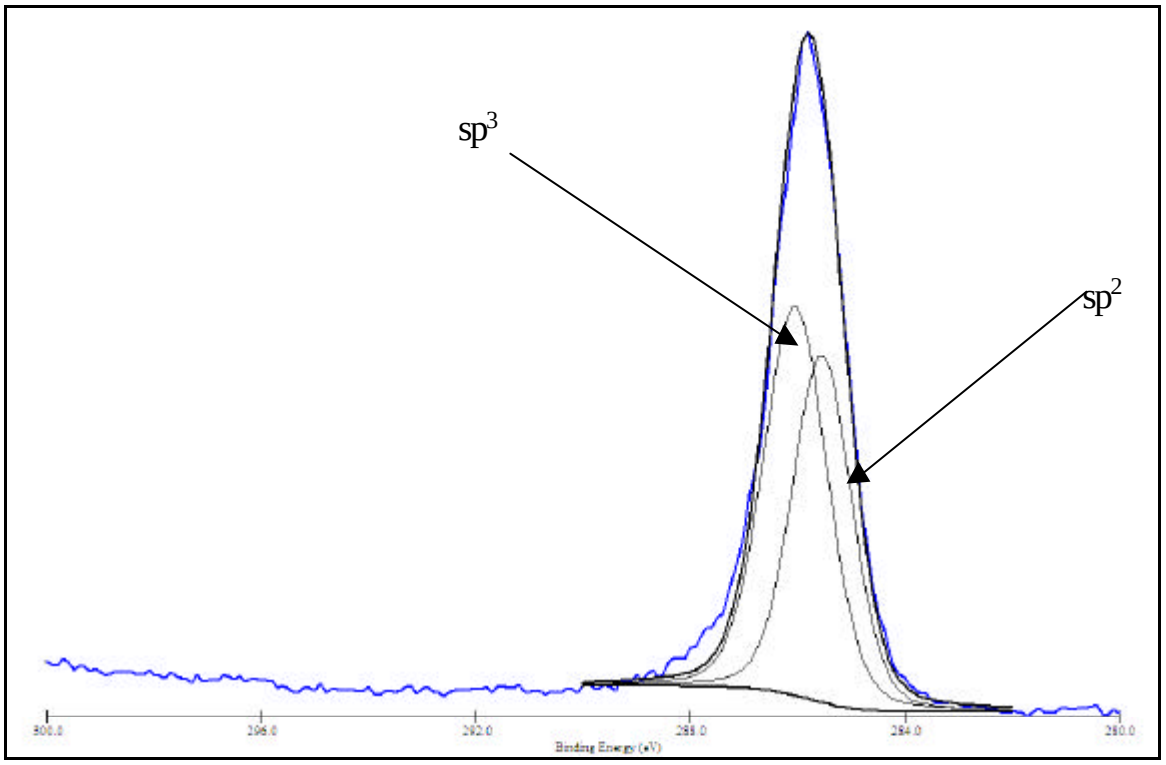

Figure 4.2: XPS Spectrum of the C 1s peak of sample JF06, fitted with the two peak method suggested by Leung *et al*[5].

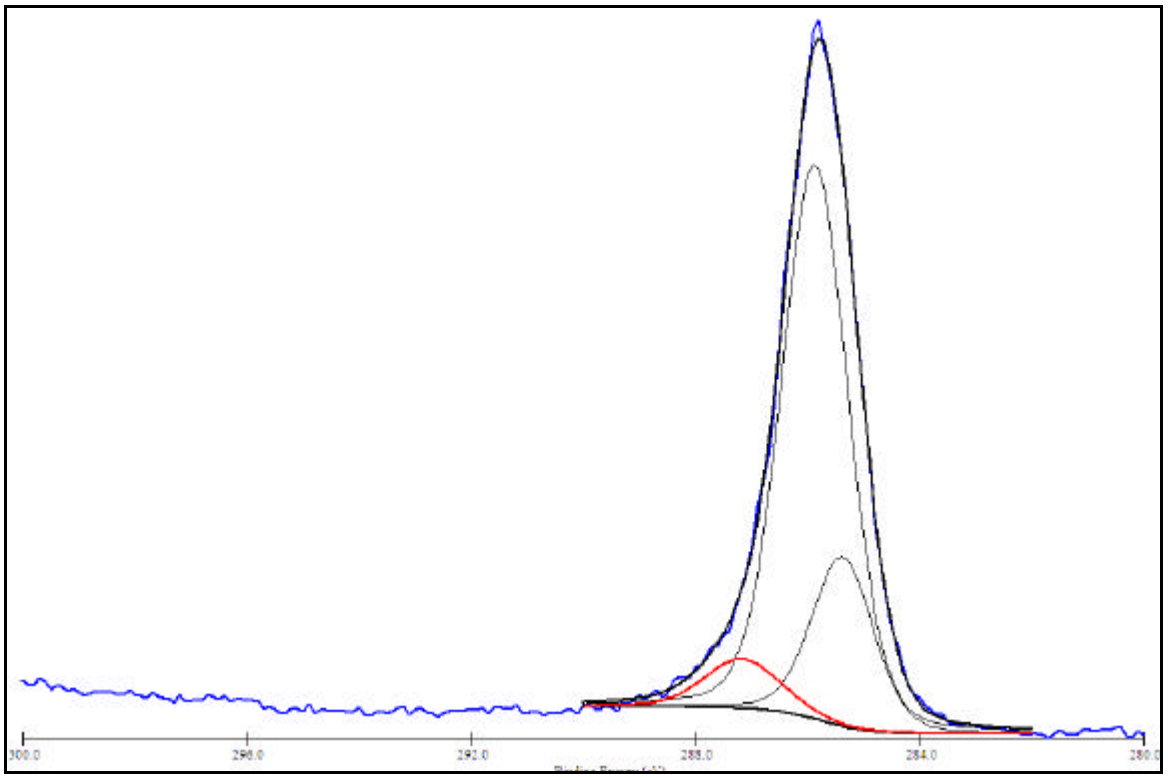

Figure 4.3: XPS spectrum of the C 1s peak of sample JF06, fitted with the third peak suggested by Merel *et al*[6].

In this study fitting with the 3-curve method always produced a better fit than with the 2-curve method. $?^2$ is a measure of the correlation of the curve fit to the experimental curve. The lower the $?^2$ value the closer a fit the fitted curves are to the experimental data. For all data in this study the data fitted by the 3-curve system had a lower $?^2$ value than data fitted with the 2-curve system.

Figure 4.4 and Figure 4.5 show the sp^3 ratio of all the films analysed found by the 3-curve and 2-curve systems, respectively. With data fitted using the 3-curve system (Figure 4.4) it can be seen that the highest sp^3 ratios within the films occur from -50 to -150 V DC-Bias. It is also seen that as the pressure increases the highest sp^3 ratios occur at higher DC-Biases. This is because as pressure increases, ions being accelerated across the sheath are more likely to collide with neutrals in the sheath

region and inelastically scatter (see chapter 2). This means to achieve a given ion energy the DC-Bias must be increased with increasing pressure. These results also agree with the results of Veerasamy and Weiler *et al*[8,9]. The films with the highest fraction of sp^3 bonding occur at ion energies of approximately 100 eV (the DC-bias of the chamber used in this study gives an approximate value for the average ion energy especially at lower pressures[10]).

The data fitted with the 2-curve method (Figure 4.5) show the same overall trend and show a maximum sp^3 ratio in the films at the same point. But it can be seen that predictable trends cannot be taken. Some scatter of data points is expected and indeed is shown on both sets of data, but the data scatter is a lot more prominent on the data fitted with the 2-curve method.

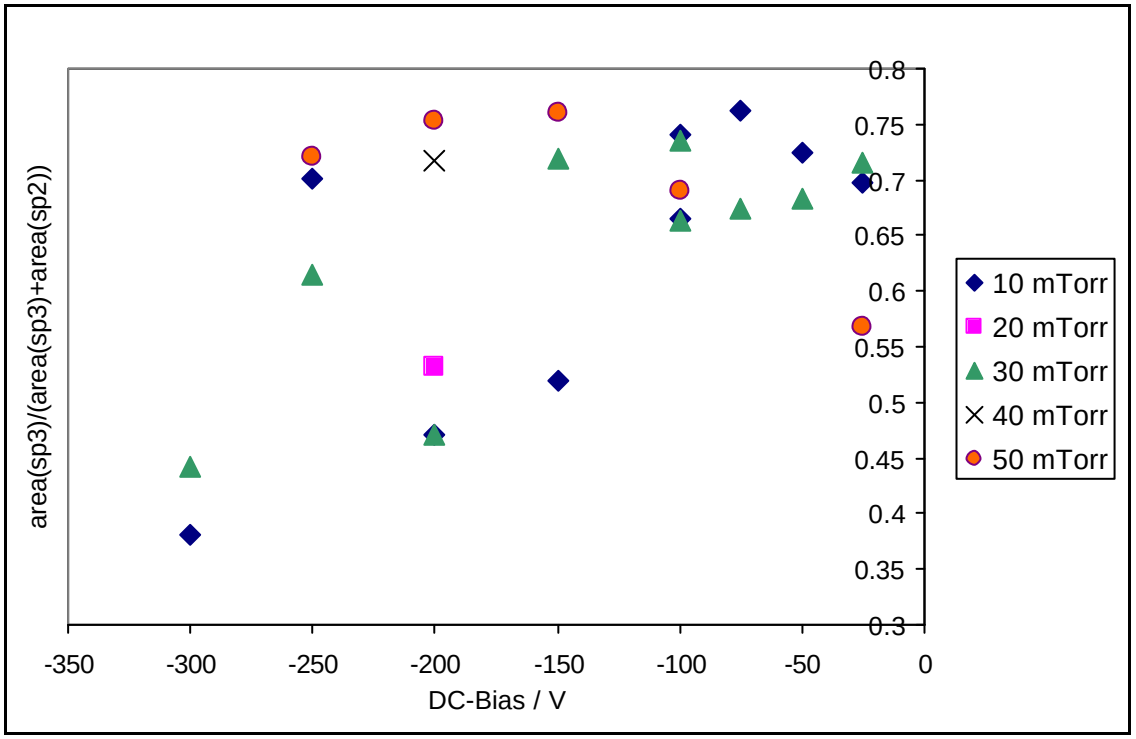

Figure 4.4: Ratio of sp^3 C-C bonding in all films from this study, these data were obtained using the 3-curve fitting method

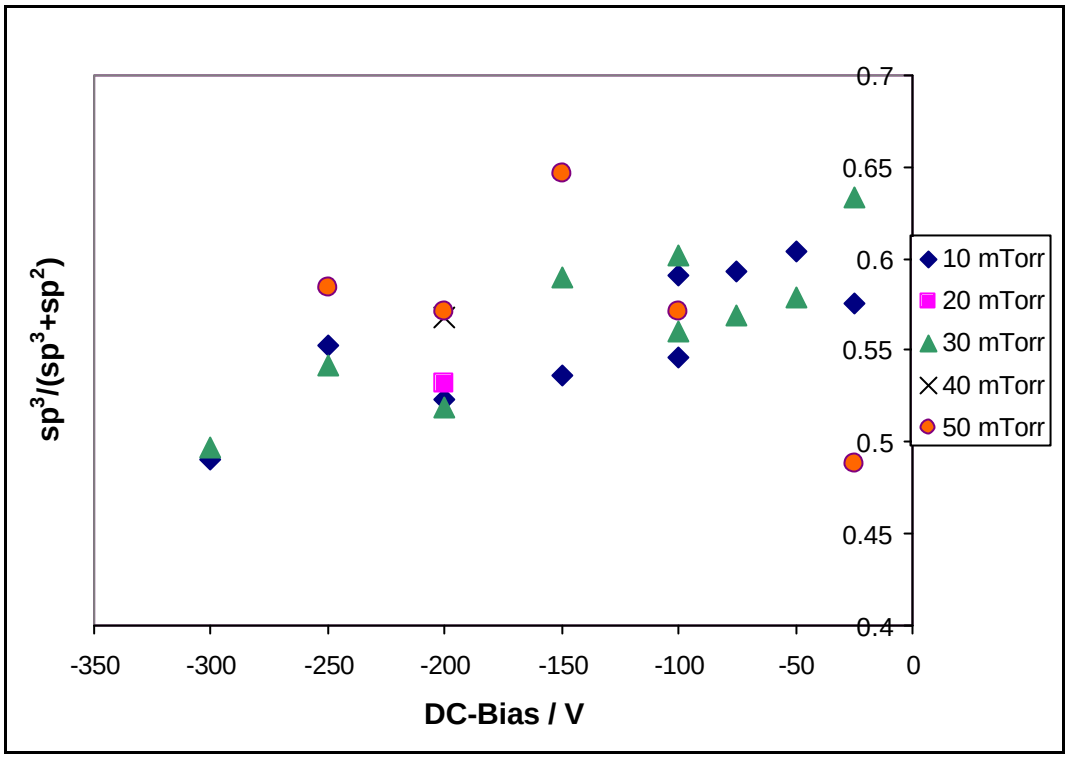

Figure 4.5: : Ratio of sp^3 C-C bonding in all films from this study, these data were obtained using the 2-curve fitting method.

From these data the chamber conditions for the growth of films with the highest sp^3 content would be with the DC-bias between -50 and -200 V and pressure between 10 and 50 mTorr. At higher DC-biases the films that are grown have a decreased sp^3 content, which would not favour the predicted structure of carbon phosphide. High pressures increase scatter across the sheath region and low pressures allow background gases to be incorporated into the film, so a medium pressure is best (20-30 mTorr).

Therefore the above chamber conditions should favour the growth of carbon phosphide with the structure predicted by Claeyssens *et al*[2]. Higher DC-biases in this range would also be sensible, because at lower DC-biases the structure of the films is polymeric and have a high hydrogen content. It has been shown by various authors

that the hydrogen content of amorphous carbon can be reduced by increasing the ion energy[8,9,11-14], thus sputtering away light hydrogen atoms. Aspects of this study have been published in Diamond and Related Materials[15].

4.2 Addition of PH_3 to the Process Gas Mixture

4.2.1 Aims

The aim of this study is to replicate and extend the work of Kuo *et al*[11,16] who produced amorphous carbon phosphide films by RF-CVD previously, with P:C ratios of 0.9:1. The properties of deposited films will be analysed, with regard to their chemical contents and their optical band gap. Post deposition annealing will also be conducted and its effect on the chemical composition and optical band gap of thin films will be assessed.

4.2.2 Deposition and Analysis Parameters

For this study all films were deposited using the chamber described in chapter 3. In this initial study all films were grown at −150 V DC-Bias, at 25 mTorr for 30 minutes. The PH_3:CH_4 ratios were varied in order to produce films with various compositions. The flow rate was kept at 30 SCCM. Films that were annealed post deposition were annealed at a pressure of $<10^{-5}$ Torr, films were annealed for 30 minutes. The film composition was analysed using XPS and SIMS. UV/Vis spectroscopy was used to find the optical band gap of the material. LRS was used to assess the long-range order of the carbon network within the thin film; the light source used in the LRS study was a 488 nm laser.

4.2.3 Results and Discussion

4.2.3.1 As-deposited films

The films exhibited a range of colours depending upon film thickness and composition. In general, the C-rich films appeared dull, but the P-rich films looked shinier and more silvery. Electron microscopy and ion beam induced secondary electron microscopy showed all the films to be smooth on a nm scale. Some of the films showed a tendency to crack and flake, especially those containing a low concentration of P. As-deposited P-containing films that were left for more than a few hours in air often cracked and delaminated. This could be prevented either by keeping the samples under high vacuum or in an evacuated desiccator. This suggests that the as-deposited films are highly reactive to components within air and are being either oxidised or hydrolysed by O_2 or water vapour respectively.

The deposition chamber electrodes were covered with a hard red coating after deposition. The coating when exposed to air produced a gas that smelt a bit like phosphine. Because of this a fume cupboard was built around the reactor. The coating was not readily sputtered away by means of an air plasma, so it was manually scrubbed after each deposition with isopropyl alcohol, acetone and water. Subsequent depositions could not be undertaken until the chamber had fully pumped down to its known base pressure. The build up of this coat caused the DC-Bias to decrease over time whilst depositing. The RF power was increased to compensate for this. It has

been shown by Kuo *et al*[11] that increasing the DC-bias kept the ion energy distribution as constant as possible and the film composition as uniform as possible.

Figure 4.6 shows an XPS spectrum of an amorphous carbon phosphide thin film. It can be seen that the XPS detects carbon, phosphorus and oxygen. Figure 4.7 shows the regions C 1s, P 2p and O 1s more closely. From the C 1s region it was found that curve fitting would be troublesome, because there are many potential bonding environments for C in this film (C-C, C=C, C-P, C=P, C-O, C=O, *etc*…), but the peak FWHM is relatively small (~2 eV). The same is true with the P 2p peak, the peak has a relatively small FWHM (~2.5 eV) compared with the number of potential bonding environments. Also there is an extra peak for each fitted peak due to spin orbit coupling. The main phosphorus peak observed is P $2p^{3/2}$ and there is another less prominent peak due to the P $2p^{1/2}$, which is always +1 eV from the P $2p^{3/2}$ peak[7]. So therefore it is only possible to quantify accurately the chemical composition of the surface of the film, not its bonding characteristics. On highly oxidised films there were two distinct P 2p peaks. The extra peak was due to P bonding with highly electronegative oxygen.

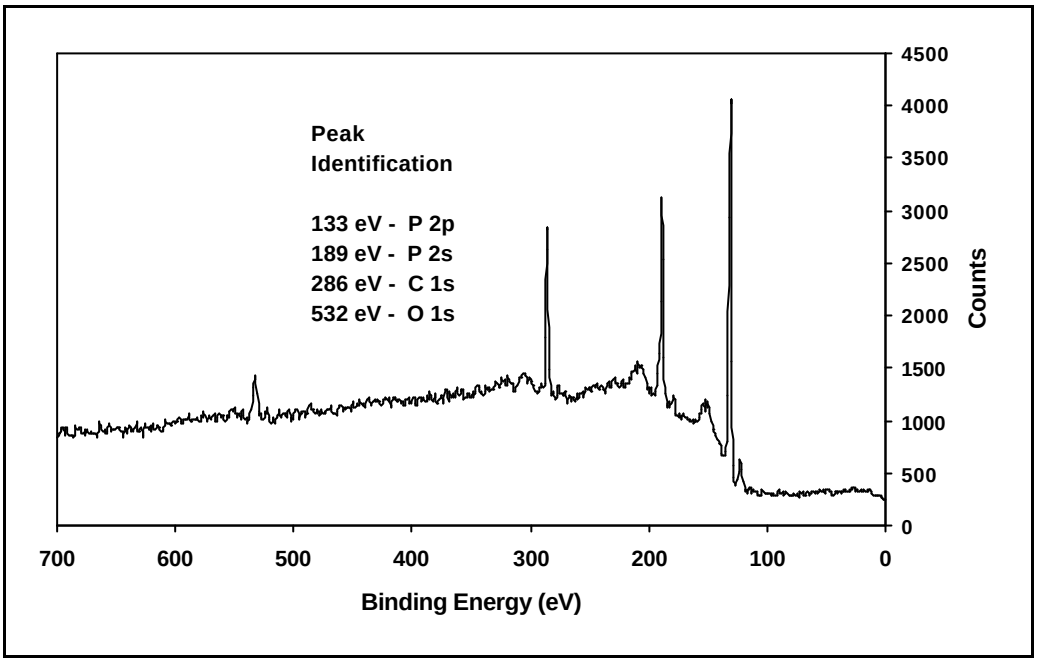

Figure 4.6: Wide XPS spectrum of an amorphous carbon phosphide thin film. This film was grown with 20% PH_3, 80% CH_4 in the gas phase with a DC Bias of –150 V for 30 minutes

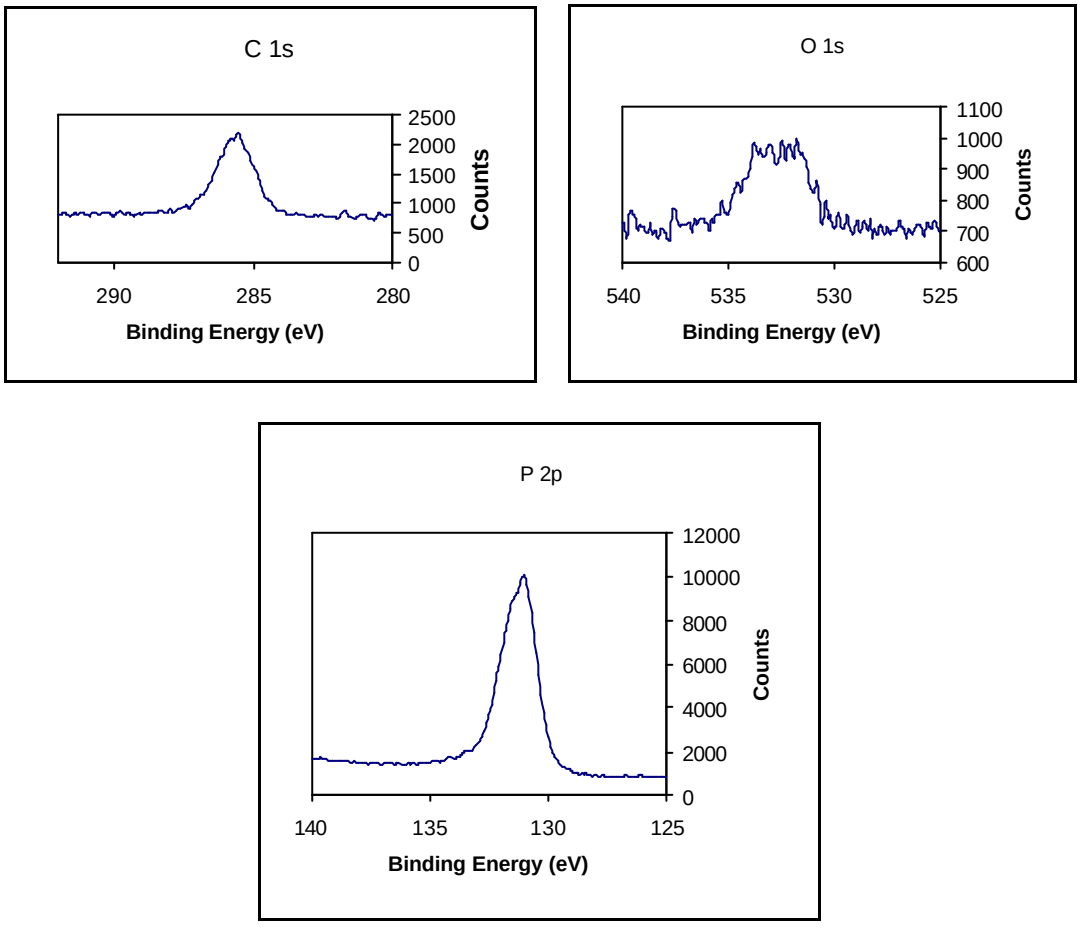

Figure 4.7: Detailed XPS spectra of the C 1s, O 1s and P 2p regions of the same amorphous carbon phosphide thin film shown above.

Figure 4.8 shows that there is a linear relationship between the P:C ratio in the as-deposited films (measured by XPS) and the PH_3 concentration in the process gases. Figure 4.9 shows that at low PH_3 concentrations, P is incorporated into the films more readily than C, but above a gas phase P:C ratio of ~2:1 (equivalent to ~67% PH_3 in the gas mixture) this trend for the apparent preferential deposition of P is reversed.

Figure 4.10 shows the growth rate of the films against the measured P:C concentration in the film. The general trend is for the growth rate to increase with increasing P content, *i.e*. with increasing PH_3 content in the input gas. Both the above observations can be explained by recalling that deposition in such RF plasma systems is a balance between the impacting species adhering to the film and the removal of surface atoms by physical sputtering or even chemical etching[17]. The increased deposition rate may simply be due to the fact that P is heavier than C and so sputters less easily, or it may be a more complicated function of the actual structure of the surface bonding for the two types of atom and the nature of the impacting species. Nevertheless, from Figure 4.8 it is apparent that films grown with the highest PH_3:CH_4 ratio contain P:C ratios of 3:1, *i.e*. the film composition is CP_3H_x (where $x \sim 0.5$, estimated by previous work by Kuo *et al*). This is the highest P:C ratio reported in a thin film.

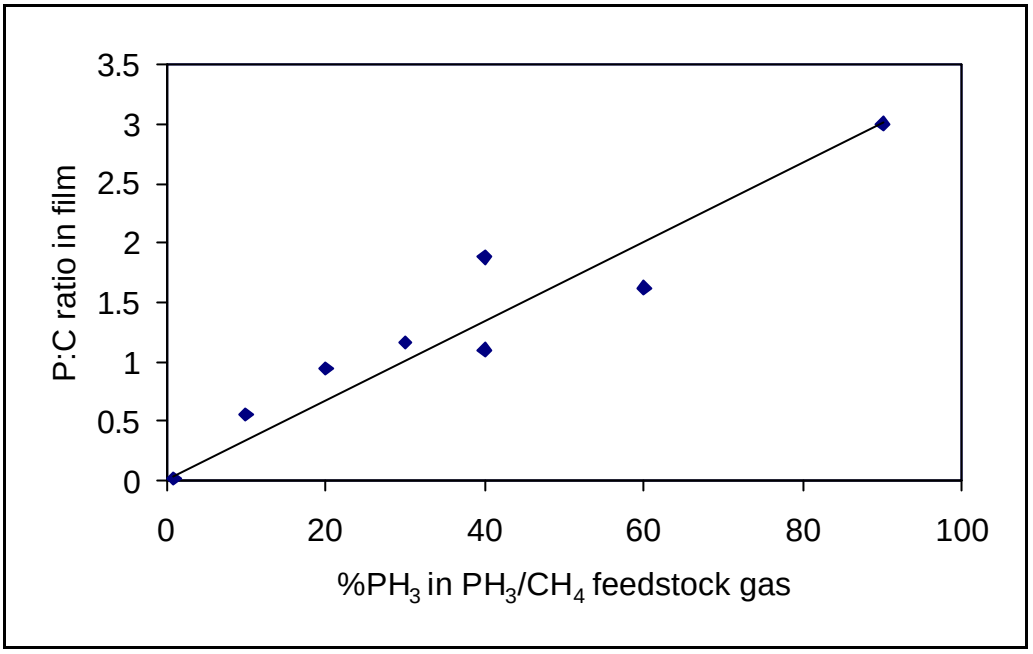

Figure 4.8: P:C ratio of several films as a function of the %PH_3 in the feedstock gas as found by XPS.

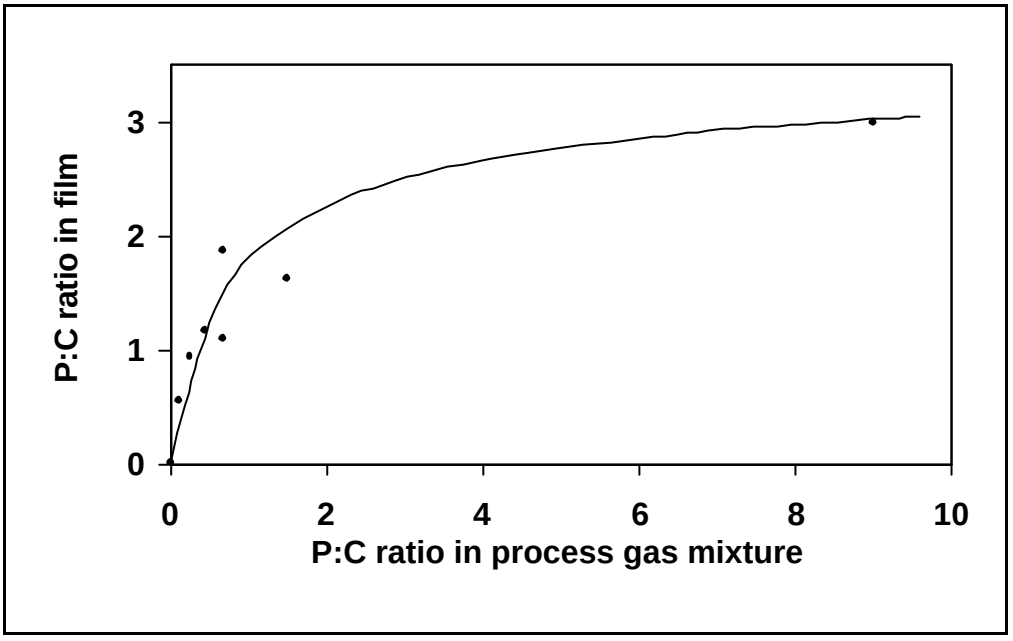

Figure 4.9: P:C content of the process gas mixture plotted against the P:C ratio in the deposited film.

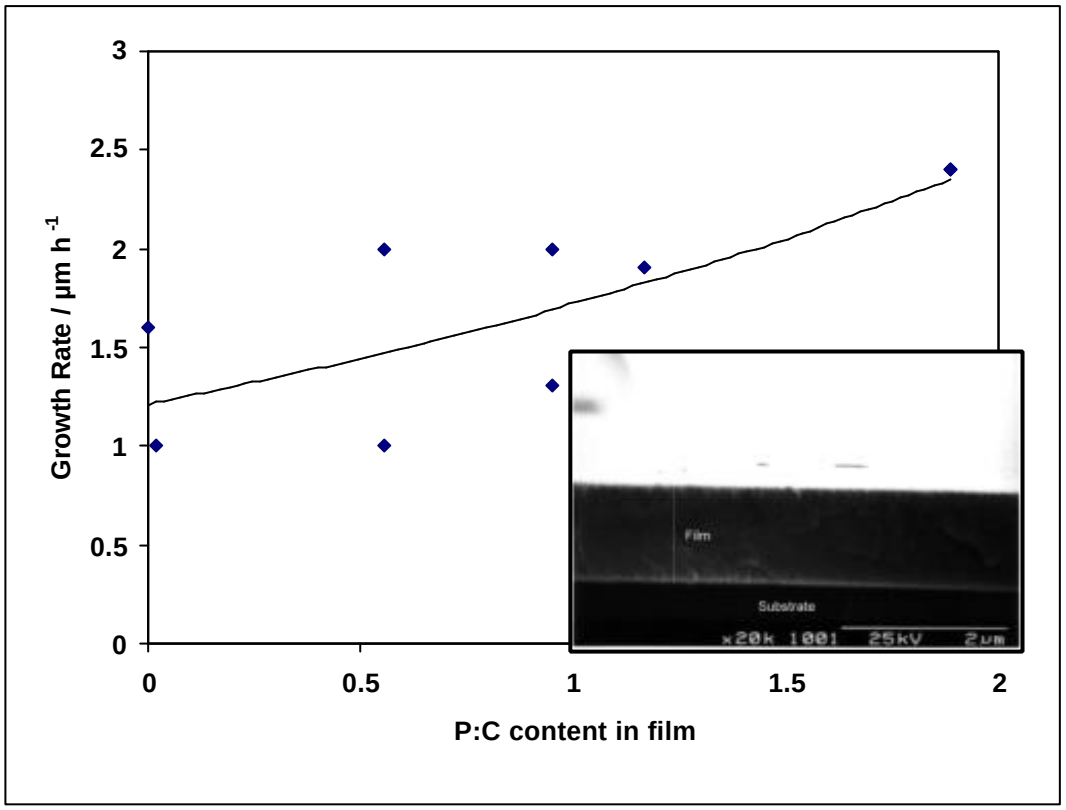

Figure 4.10: The growth rate of amorphous carbon phosphide films grown in this study (measured by SEM) against the P:C content in the film as measured by XPS, the inset is an SEM of a cross section of an amorphous carbon phosphide film.

Figure 4.11 and Figure 4.12 show an Auger Electron Spectrum (AES) of an amorphous carbon phosphide film grown in this study. Shown are a standard spectrum and a differentiated spectrum. The AES may be quantified by calculating the area under each of the curves (in the non-differentiated spectrum), or calculating the peak heights (in the differentiated spectrum) and multiplying by a sensitivity factor. It can be seen that the peaks are rather broad, but to get reasonable peaks the surface layer had to be removed by ion etching. This means that absolute C-P bonding concentration information may not be accurate. This technique was used to confirm the quantification of XPS (which it did successfully to within 5%). It was not used routinely for analysing films as it was time consuming and the sample charging on the surface layers meant that meaningful spectra were difficult to accumulate.

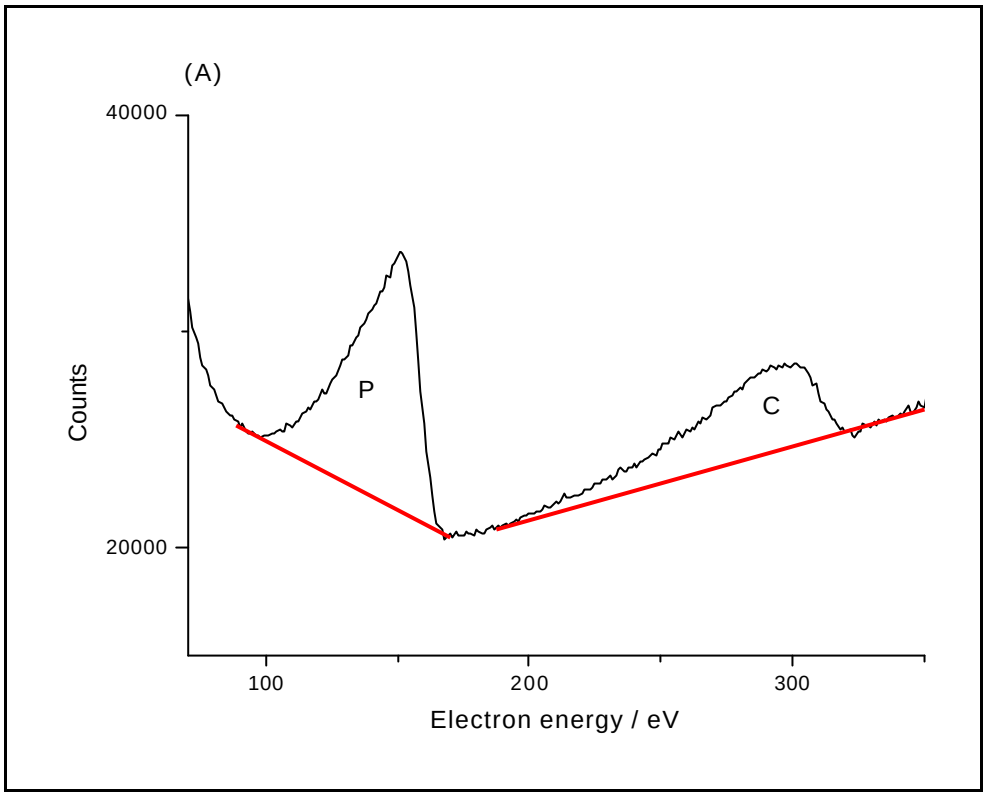

Figure 4.11: AES of an amorphous carbon phosphide film, grown from a 60% mixture of PH_3 in CH_4, at a DC-bias of –150 V. The red lines show how each type of plot are quantified.

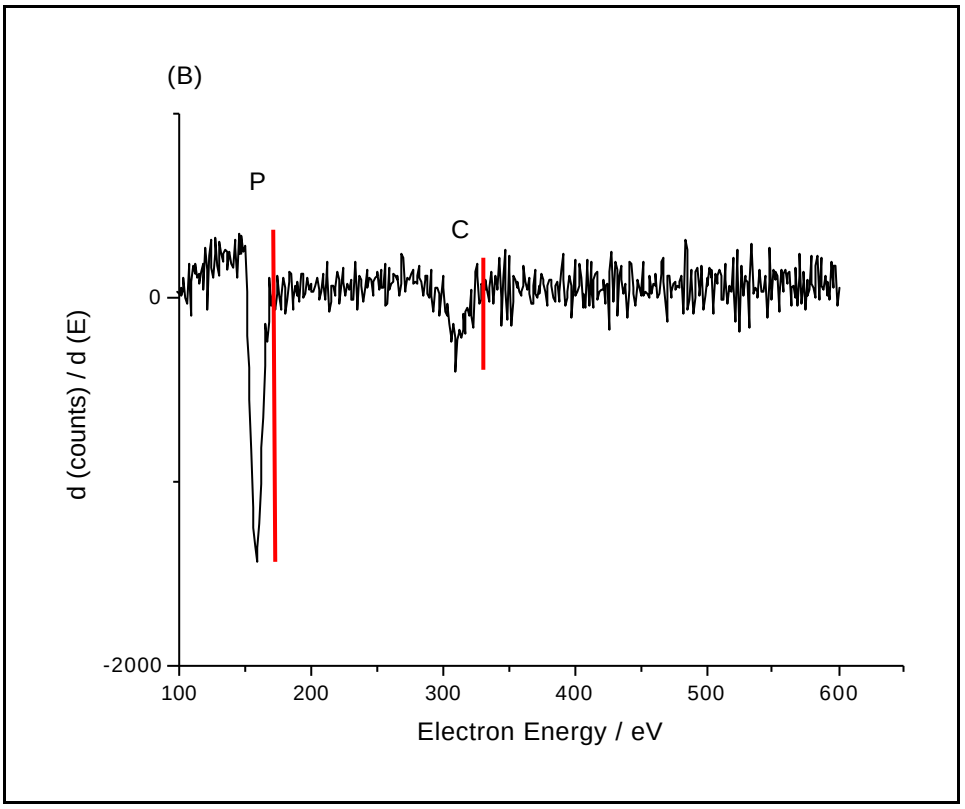

Figure 4.12: A differentiated AES of the amorphous carbon phosphide film described above. The red lines show how each type of plot are quantified.

Figure 4.13 shows a SIMS spectrum of an amorphous carbon phosphide film grown in this study (there is an identification table for the peaks in Table 4.2). It can be seen that there are a large number of carbon, phosphorus, hydrogen and oxygen containing species. It must be recalled that SIMS is not a quantitative technique, it is semi-quantitative at best. The most encouraging result is the large peak at *m/z* 43 AMU, which corresponds to CP and shows that C and P are bonding together. The SIMS results also show the presence of oxygen containing species. But as Figure 4.14 shows the SIMS depth profile reveals that there is only significant oxidation of the surface layers. The depth profile also shows that most of the CP bonding is below the as-deposited surface. This indicates that the surface oxidation is mainly due to the surface phosphorus reactions with either air or water. The spectrum shown in Figure 4.13 does not show a peak for hydrogen, but it has been detected in all films grown in this study. The reason that it is not shown on the spectrum is due to the step size on the spectrometer, lower mass peaks are thinner and with a step size of 0.1 AMU the H peak is easily missed. Previous studies by Kuo *et al*[11,16] have estimated the H content to be around 10%.

Figure 4.15 shows a SIMS element map. This shows that most of the oxidation is on the surface and that most CP lies beneath the surface of the film. It is noted that in all P containing films SIMS reveals the presence of O at low levels (estimated to be <1% of the film composition by the magnitude of drop in the SIMS signal compared to the XPS data), throughout the bulk of the film. This could be due to (a) trace oxygen impurities in the PH_3 gas supply, (b) residual oxygen being present in the deposition chamber due to the relatively high base pressure (0.1 mTorr compared to a process pressure of 25 mTorr), or alternatively (c) despite precautions, the film still

undergoing oxidation/hydrolysis during its brief contact with air, with the porous nature of the films allowing the oxidation to propagate throughout the bulk. Another explanation might be that since the levels of O are only just above the background detection limit for SIMS and XPS, they may result simply from reaction of the film with O-containing diffusion pump oil vapours present in the analysis chambers – and thus be an artefact of the analysis rather than the deposition.

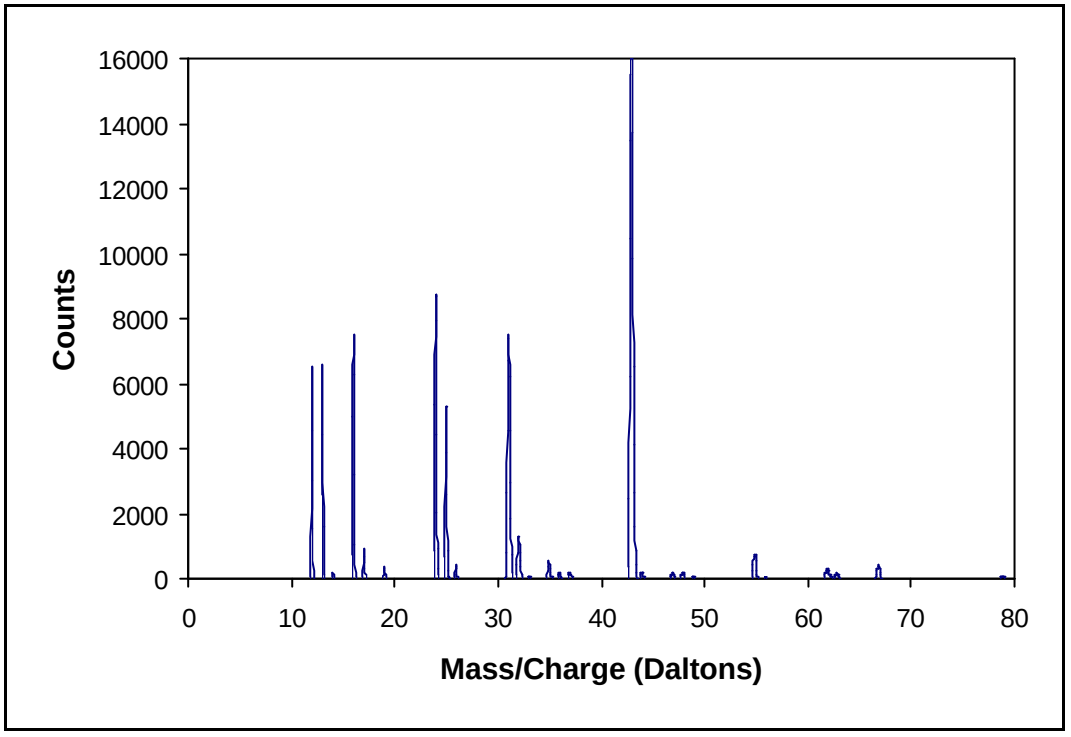

Figure 4.13: SIMS spectrum of a P containing film. This film was grown with 30% PH_3 in the gas phase, XPS studies have shown that the composition of the film is 43.07% C, 50.233% P and 5.296% O.

Mass/Charge (Daltons)	Identification
1	H
12	C
13	CH
14	CH_2
15	CH_3
16	O
17	OH
18	H_2O
19	F
24	C_2
25	C_2H
26	C_2H_2
27	C_2H_3
31	P
32	PH
33	PH_2
34	PH_3
35	Cl
43	CP
47	PO
55	C_2P
63	PO_2
67	C_3P
79	PO_3

Table 4.2: Identification table for ions detected in SIMS.

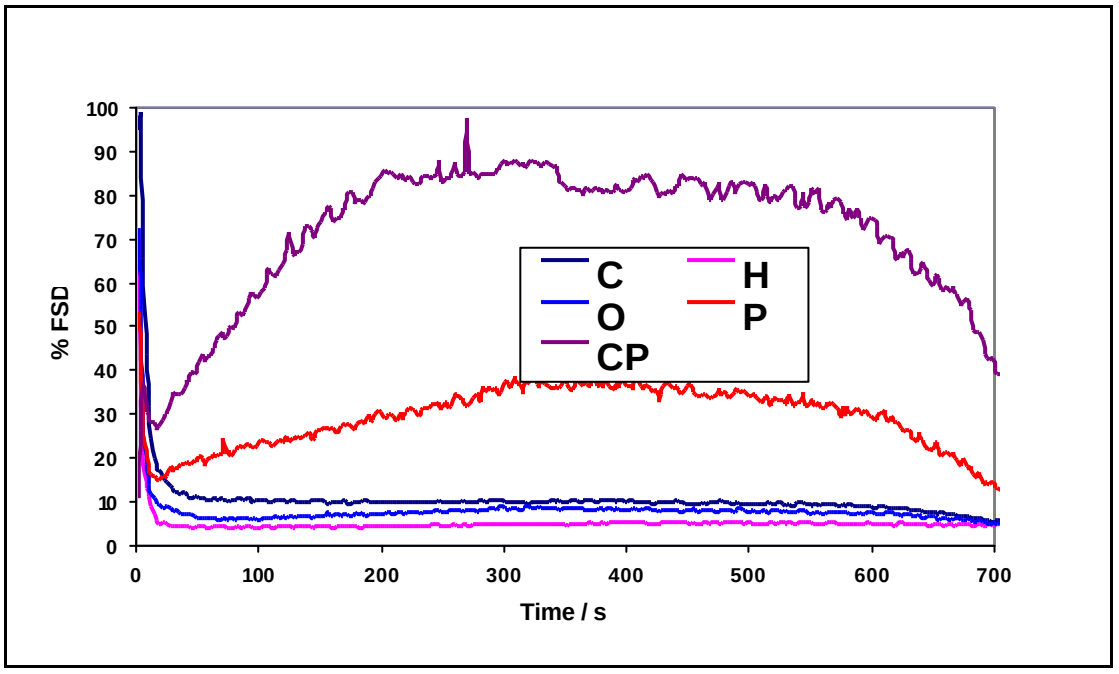

Figure 4.14: SIMS depth profile of an amorphous carbon phosphide film.

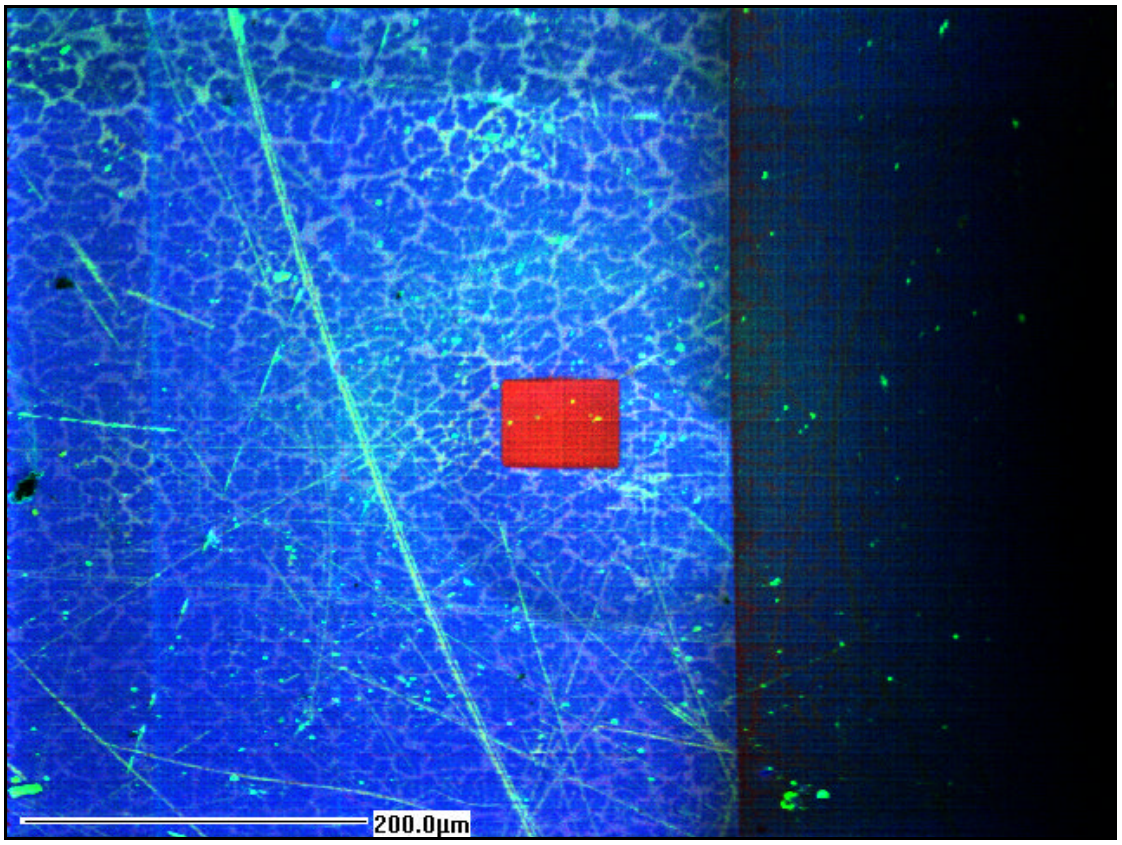

Figure 4.15: SIMS elemental map. Blue is *m/z* 12 (C) green is *m/z* 16 (O) and red is *m/z* 43 (CP). The red patch in the middle is a depth profile pit. The dark area on the right is a subsurface analysis area, which has not penetrated as far as the depth profile pit.

Figure 4.16 shows the LRS spectra from various films containing different P:C ratios, it can be seen that as the P:C ratio increases the band shown becomes less prominent, this is the same as found by Kuo *et al.*, this is due to the ordered graphite band (G-band) becoming less prominent with a higher concentration of P in the gas phase and hence in the film. This is consistent with a decrease in the number of C-C bonds as P is added. This could be due to the formation of more C-P bonds in place of the C-C bonds. Evidence for this has been obtained from SIMS analysis of these films, which gives a plethora of peaks due to C_xP_y fragments (see Figure 4.13), suggesting that there are definite C-P bonds within the film. Alternatively, the decrease in size and increase in width of the G-band might suggest that the effect of P incorporation is simply to amorphise the film and reduce the long range order - in other words the P is

simply ‘diluting’ the carbon network preventing the formation of extensive C-C structures.

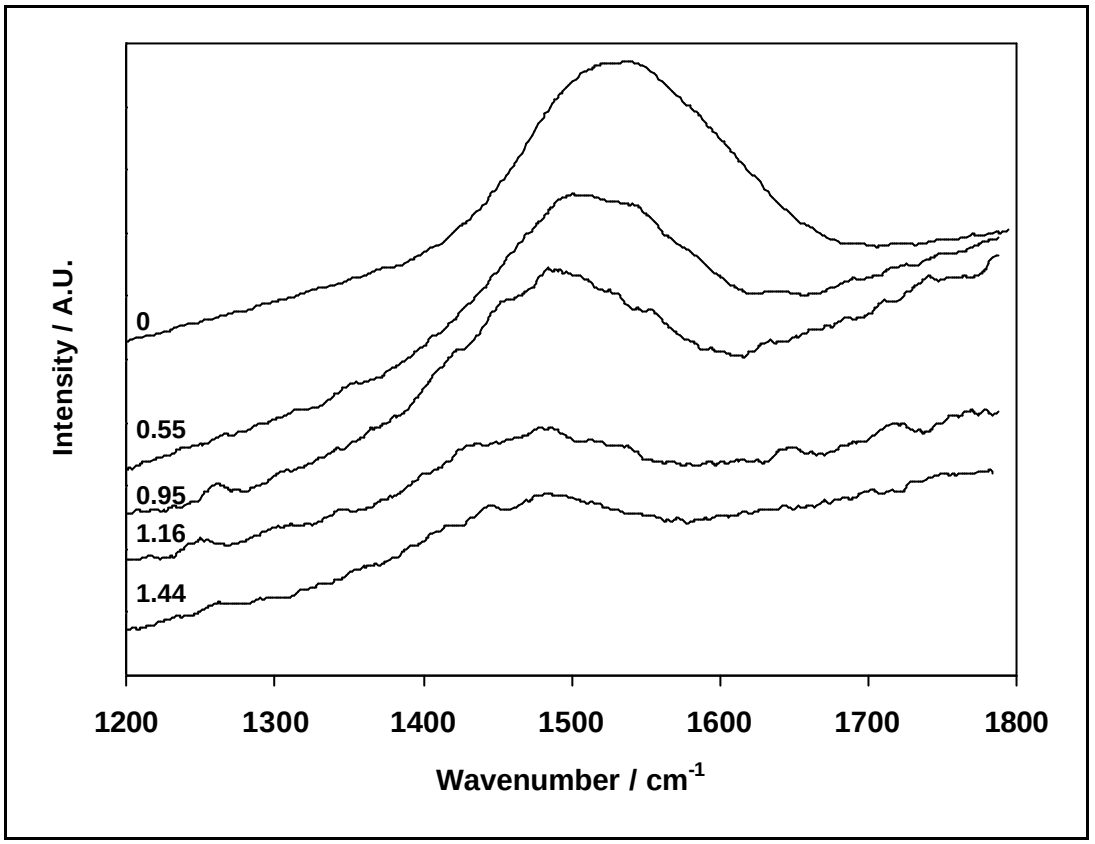

Figure 4.16: Laser Raman Spectra of amorphous carbon phosphide and amorphous carbon films with various P:C ratios (shown above each spectrum).

Figure 4.17 shows an example of an UV/Visible absorption spectrum for a film containing a P:C ratio of 1:1, along with the Tauc extrapolation used to obtain the optical band gap. The curved nature of the absorption profile leads to a fair degree of subjectivity in the position of the extrapolation line and hence uncertainty in the estimation of the band gap. Also, absorption at wavelengths smaller than the estimated Tauc band gap suggest that these films have a great many mid-band gap states, which again emphasises their amorphous, defective nature.

Figure 4.18 shows the estimated Tauc band gap for films containing various P:C ratios and show values similar to those for the P-doped films of Veerasamy *et al*[18]. The trend is for the optical band gap to decrease with increasing P:C ratio in the film. This appears to contradict the findings of Kuo *et al*[11,16], who found that for P:C ratios of 0.1-0.9 the optical band gap increased to ~3.2 eV. The difference in the two observed trends may be due to the highly air sensitive nature of these high P-content films. Unless extreme care is taken to prevent oxidation/hydrolysis of the films following deposition (as in the present work), the films change in composition and the measured properties become unrepresentative of the original as-deposited film.

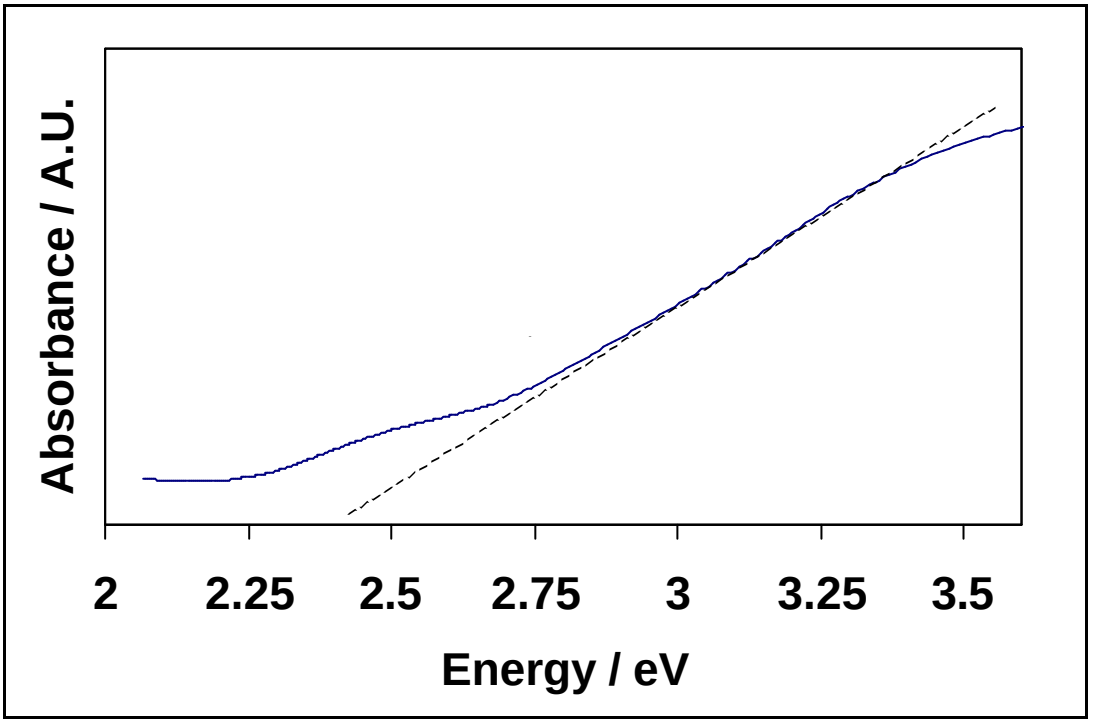

Figure 4.17: Example of a UV/Vis spectrum of an amorphous carbon phosphide film grown on quartz. The straight line is an example of a Tauc type plot, which gives an estimation of the optical band gap of the material.

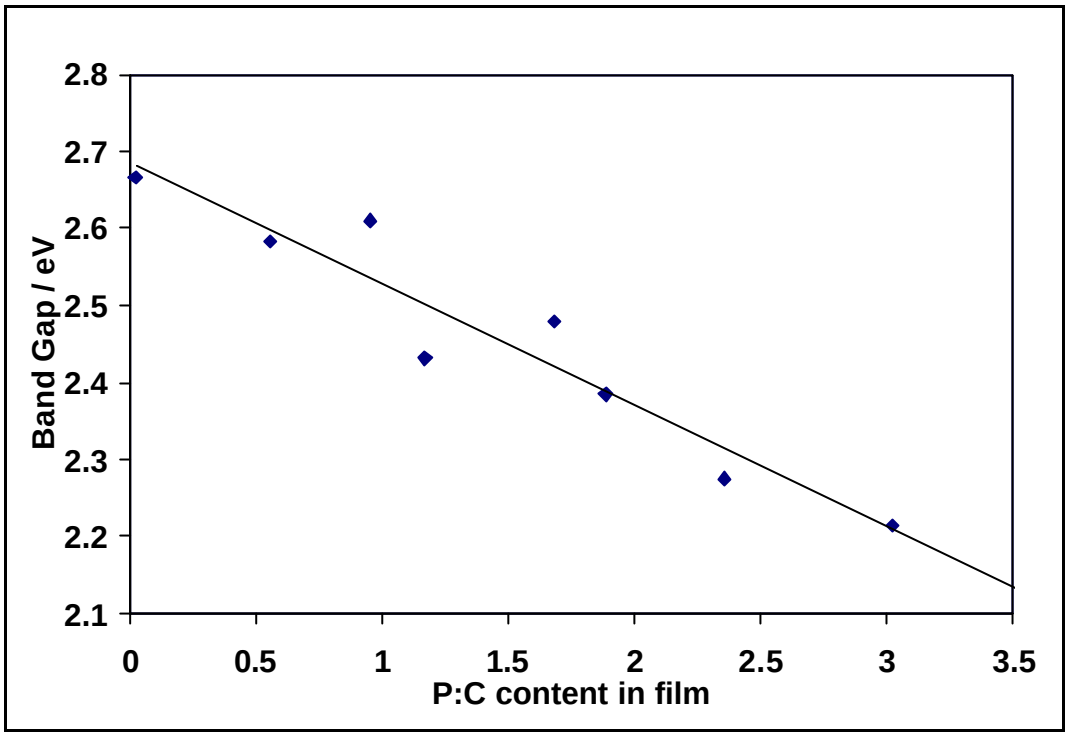

Figure 4.18: The calculated optical band gap (by the Tauc method) of amorphous carbon phosphide films plotted against their P:C content.

Alternatively, it is noted that the present films were almost certainly deposited at significantly higher ion impact energy than in the previous work. Calculations based on the model of Field *et al*[19] for RF reactors similar to the one used here, lead to an estimate of the plasma sheath thickness, ~5 mm, which is similar to the ion mean free path at the process pressure of 25 mTorr. Thus, ions will suffer few collisions on their path through the sheath, so the average energy of ions impacting the substrate surface for these conditions can be calculated as ~100 eV. Comparing this with the values from Kuo *et al.*'s work, where a higher pressure (60 mTorr) was used, the ion mean free path is calculated at ~1.5 mm which is about 3.5 times less than the estimated sheath thickness at this pressure. In the earlier work, therefore, collisions within the sheath will have significantly reduced the energy of the impacting ions. Using an estimate for the spread of energies due to sheath collisions based on the model of May *et al*[20], it is calculated that for Kuo's process conditions the average ion impact energy

on the substrate was only ~40 eV. Thus, it would not be surprising if the two types of film have different structures and compositions and therefore exhibit different trends. Figure 4.18 illustrates that the band gap of the present films can be tuned in a systematic manner from 2.1 to 2.7 eV – which may have implications if these films are to find application in electronics or optoelectronics.

Some films were also analysed using XRD, the results are not shown as no crystalline peaks that could be assigned to carbon phosphide were found. This means that the films were amorphous.

4.2.3.2 Annealed films

Films that were annealed sometimes exhibited different colour to the as-deposited films. For example, it was usual for green films to become red after annealing. If an as-deposited film was silver, it stayed silver after annealing. It was thought that this was due to a change in structure of the film, or the thinning of the film and that this would not be necessarily noticed in a very thin as-deposited film. At temperatures in excess of ~350 ºC the thin film sometimes melted. Upon cooling islands of a brown solid were found on melted films. It must be remembered that some forms of phosphorus have a relatively low melting point (44 ºC for white phosphorus, 590 ºC for red phosphorus and 610 ºC for black phosphorus[21]) especially compared to carbon. It was also found that annealed films did not delaminate unlike as-deposited films. This simple observation shows that either annealing removes weakly, or non-bonded species from the film (such as PH_3), or it causes these species to bond more strongly.

Figure 4.19 shows a graph of the P:C ratios within a set of films deposited with exactly the same parameters, but annealed at various temperatures. It can be seen that the P:C ratio in the film decreases at higher annealing temperatures. This is thought to be due to the removal of captured phosphine gas and also the removal of weakly bonded phosphorus species from the structure. Along with the reduction of the P:C ratio was a vast increase in the oxidation of the surface of the films. As the pattern of any graphs produced of this effect was random it was thought that this was due to sample handling issues.

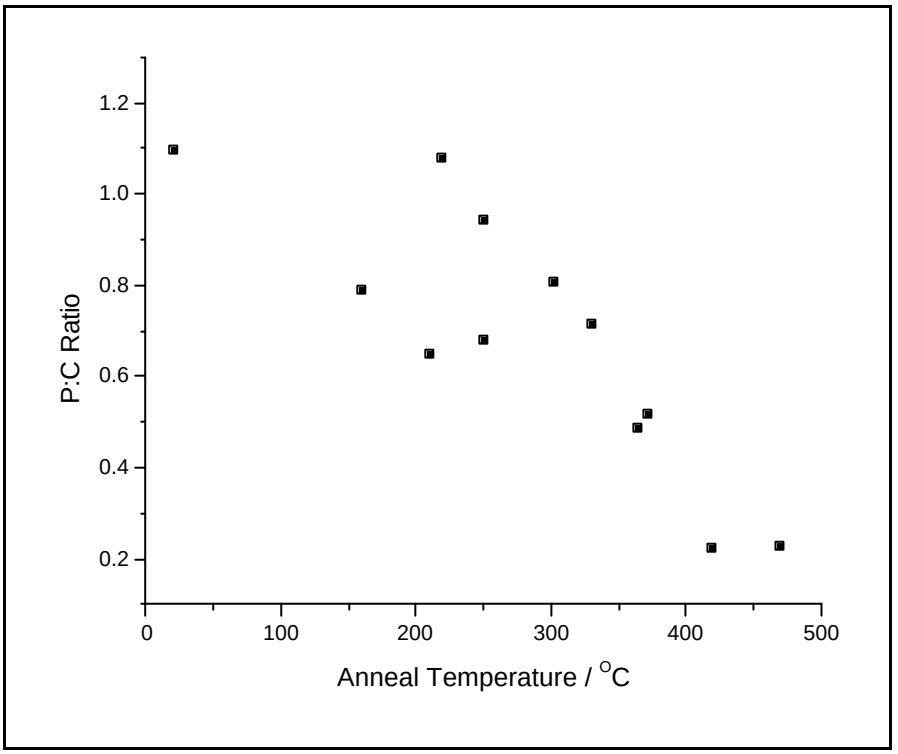

Figure 4.19: Graph showing the post deposition anneal temperature against the P:C ratio (measured by XPS) of amorphous carbon phosphide films, deposited with 25% PH_3 and 75% CH_4 with a DC-bias of –150 V. All films were annealed for 30 minutes. The point at 21 °C is as-deposited.

Figure 4.20 shows the effect of annealing films at 300 °C for half an hour on the optical band gap of the film. It shows that compared to the as-deposited films the band gap is slightly higher in all cases. This is direct evidence for the changing of the structure in the thin film when they are annealed.

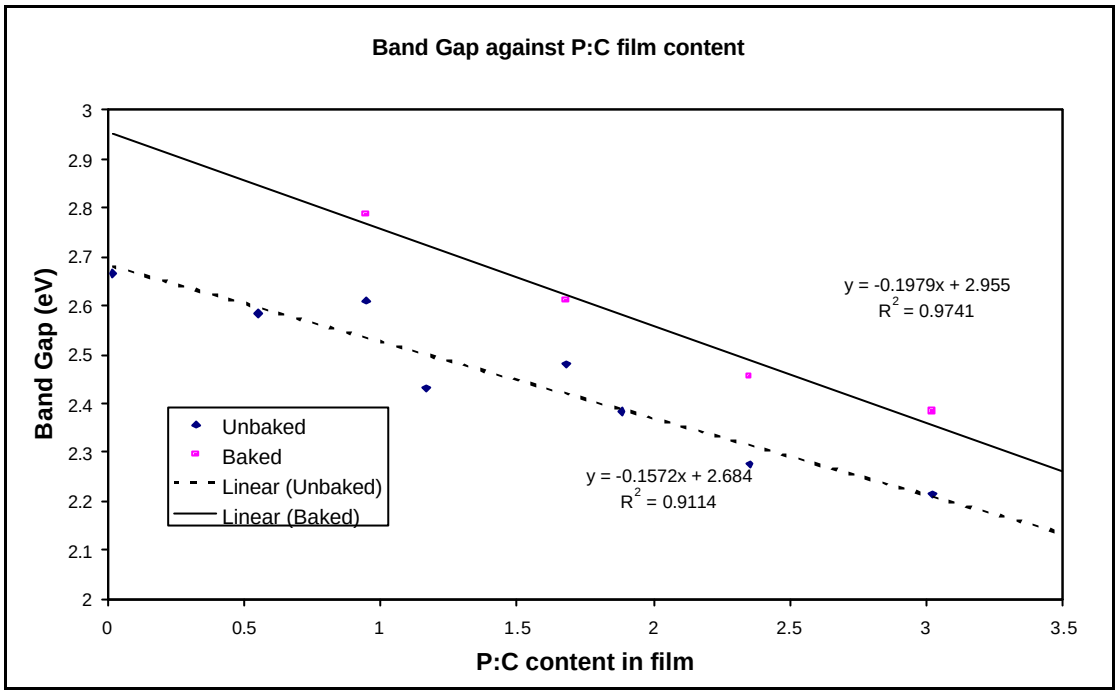

Figure 4.20: The optical band gap of annealed and as-deposited amorphous carbon phosphide thin films.

Figure 4.21 shows SIMS depth profiles of an as-deposited amorphous carbon phosphide film and an annealed amorphous carbon phosphide film. It can be seen that the trends of species throughout the film are similar. However if the number of counts of P against the number of counts for CP are calculated for the as-deposited and annealed films it is found that the annealed film has a higher CP:P ratio (in this case the as-deposited film has a CP:P counts ratio of ~20, with the annealed film this ratio is ~24). As previously mentioned, it is not possible to accurately quantify the SIMS, but these results show that even though, as shown by XPS, the P:C ratio within the films decreases at higher annealing temperatures, there is some enhancement of the CP:P ratio, which suggests that the phosphorus being removed is non-bonded phosphorus. Annealing almost certainly increases the bonding between carbon and phosphorus, this is evident because in addition to the increase in the CP:P counts ratio the optical band gap varies suggesting that the chemical structure of the film changes.

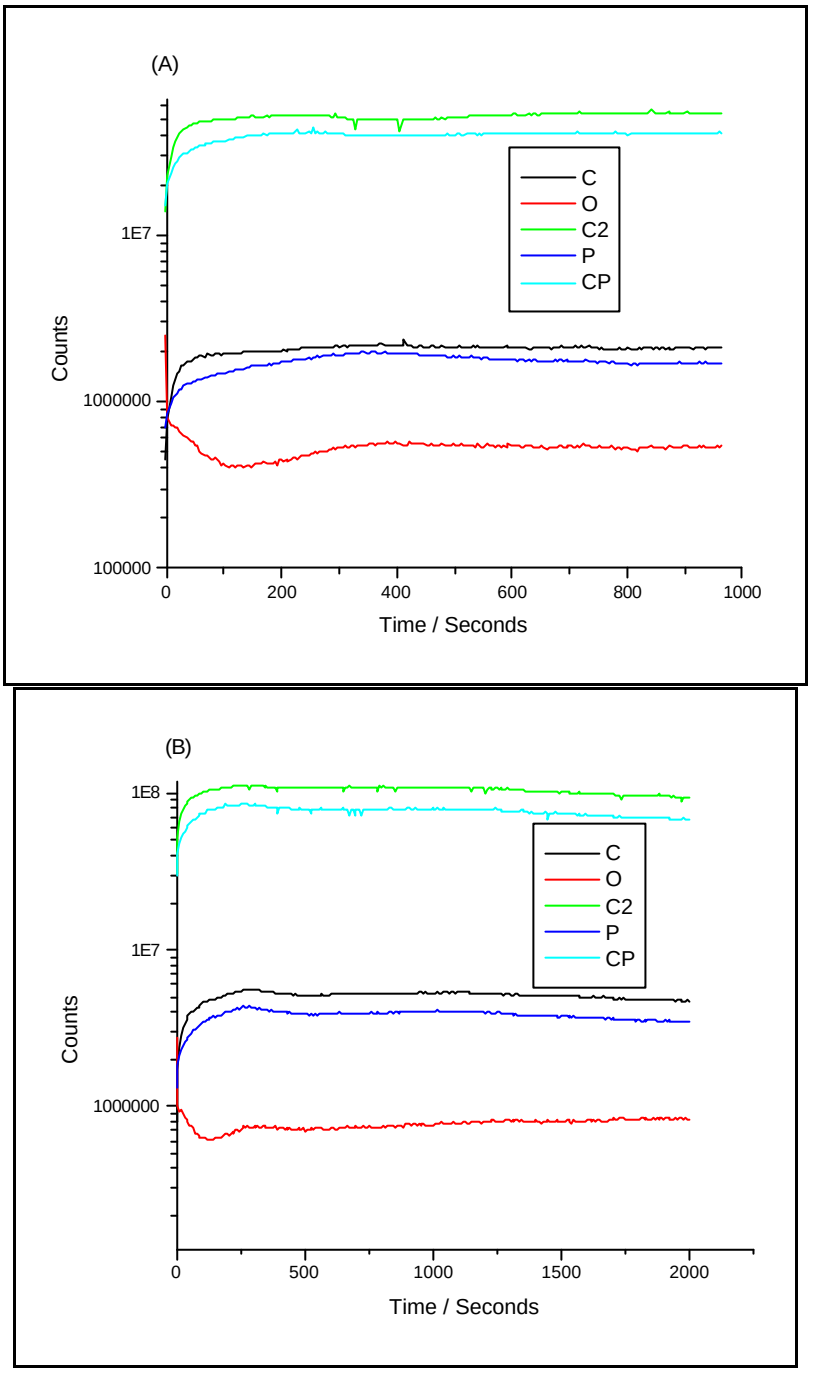

Figure 4.21: Depth profiles of (A) an as-deposited amorphous carbon phosphide film and (B) an amorphous carbon phosphide film, annealed at 210 ºC.

At this point it is important to clarify the surface modification of the film by ion etching. If this study was concerned with the absolute concentrations of species it would not be correct to use the number of counts of various species as their concentration. An obvious example of this would be the CP species detected by

SIMS. How do we know that this is not just formed as a result of the ion beam bombardment in SIMS? It is likely that the Ga ion beam used in SIMS would form some CP bonds, as it will be causing thermal spikes and will transfer kinetic energy to the surface, which may cause surface and subsurface re-arrangements. But firstly the CP peak is the largest in most SIMS spectra taken and secondly the CP:P ratio would not increase after certain treatments, such as annealing, the CP:P ratio would most likely remain the same, or similar. Therefore, it is correct to use the relative difference between counts for one species compared to other counts from another specie taken in the same spectrum to discuss relative amounts of CP bonding and relative amounts of other species.

XRD spectra were taken of annealed films, but no peaks that could be assigned to crystalline carbon phosphide were found. It is clear that annealing whilst changing the bonding characteristics of the films did not increase the long-range order of the films.

The above results show that films can be grown with high P:C ratios (of up to 3:1) and beyond. The limiting factor in this study was that at high PH_3 concentrations the chamber was contaminated with a hard coating which was very difficult to remove. It was also thought that it was unsafe to only use PH_3 in the deposition system. The films that were grown had an optical band gap that varied linearly with gas mixture, but were still amorphous. It was shown that post deposition annealing could increase the stability of these films and change the structure (and hence the optical band gap) of these films. Unfortunately these films are amorphous and still contain a small

proportion of hydrogen (estimated at around 10%). Aspects of this study were published in Diamond and Related Materials[22].

4.3 Variation of the ion energy and its effect on the deposition of amorphous carbon phosphide thin films

4.3.1 Aims

The aim of this study is to vary the ion energy of ions crossing the sheath and study the effects on the deposited film. The films were grown with a gas flow of 30 SCCM with the gas mixture set as 30% PH_3, and 70% CH_4, at a pressure of 25 mTorr, deposition times were for 20 minutes.

4.3.2 Deposition and Analysis Parameters

Films were deposited as described above, varying the RF-Power varied the ion energy. The DC-bias was kept constant by varying the RF-power. The top-hat chamber design, with cathode : anode electrode area ratios of about 3:1, was such that under these reaction conditions the DC-bias was a good measure of the average ion energy[10].

The P:C ratio was measured on the Fisons VG Escascope described in Chapter 3. An attempt at improving the resolution of the XPS was made at the Daresbury Synchrotron Light Source. It will be shown later this was unsuccessful. SIMS spectra were taken using the instrument described in Chapter 3. UV/Vis was used to

obtain the optical band gap of deposited films. SIMS was used to assess the C-P bonding.

4.3.3 As-deposited films

The films were coloured in appearance; those deposited with DC-biases of up to ~-250 V had a green/red appearance, whereas films deposited at higher bias values were either transparent or silver in colour. Imaging focused ion beam analysis was used to measure the film thickness. This showed that films deposited at bias values greater than -250 V were much thinner (typically 200-400 nm) than films grown at lower biases (typically >500 nm) for deposition times of 30 minutes.

SIMS depth profiles similar to that shown in Figure 4.14 show the composition of the bulk is relatively uniform below the point at which the CP signal plateaus. The ratio of P:C and PC:P counts (taken at or below this point) can give an indication of the type of bonding present in the films as a function of deposition conditions. Care was taken to ensure that the SIMS was calibrated to detect H; it was found that just below the surface the H level was below the detection limit of the SIMS. Figure 4.22 shows a plot of the P:C ratio measured by XPS of films grown at various bias voltages. The amount of P incorporated into the film decreased as the DC bias increased (became more negative). The reason for this is unclear, but it may be due to preferential sputtering of weakly bonded PH_x (x = 0-3) species from the surface compared to the more strongly bonded CH_x (x = 0-3) species.

Figure 4.23 and Figure 4.24 shows that the CP:P and CP:C ratios increases with increasing DC bias. The CP:P and CP:C ratios are not direct measures of absolute

concentration, but rather measures of relative counts and give an idea of the proportion of P that is directly bonded to C in the film, as opposed to phosphorus that is present as individual non-bonded P atoms or P_x clusters. Figure 4.23 shows that at higher DC bias values, even though the absolute concentration of P is decreasing within the film, the P that remains is that which is bonded to C. Figure 4.24 shows that the proportion of C is increasing (as shown by XPS) the CP ratio is also increasing. Therefore, increasing the ion impact energies does, indeed, increase the C-P bonding within the film.

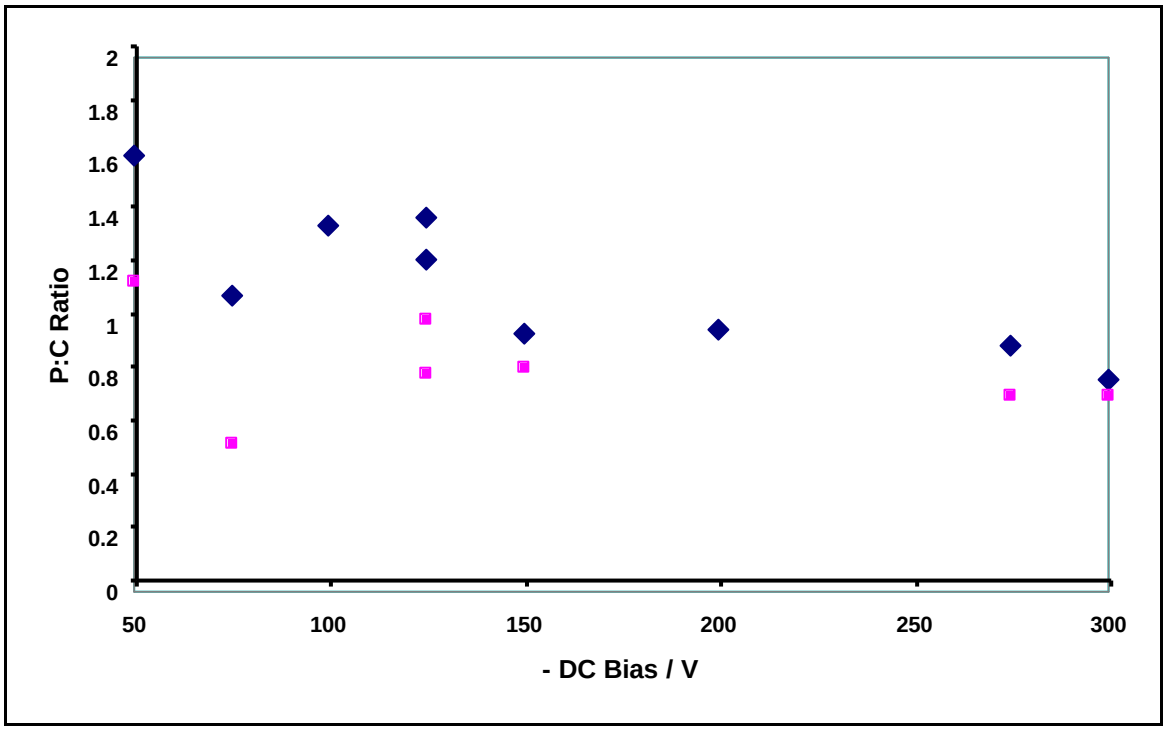

Figure 4.22: P:C ratios measured by X-ray photoelectron spectroscopy (XPS) plotted against the (negative) DC bias voltage. The black diamonds represent as-deposited films, the purple squares represent annealed films.

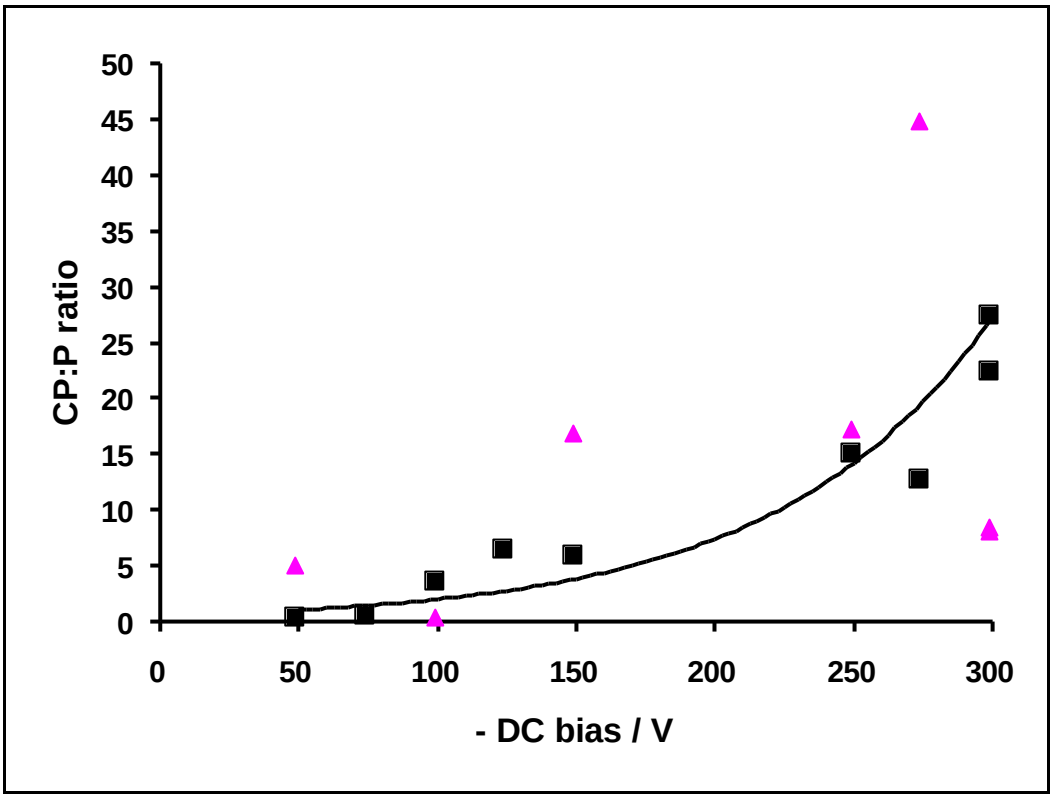

Figure 4.23: CP:P ratios for films measured from SIMS depth profiles plotted against deposition DC bias. The black squares represent as-deposited films, the purple triangles represent annealed films.

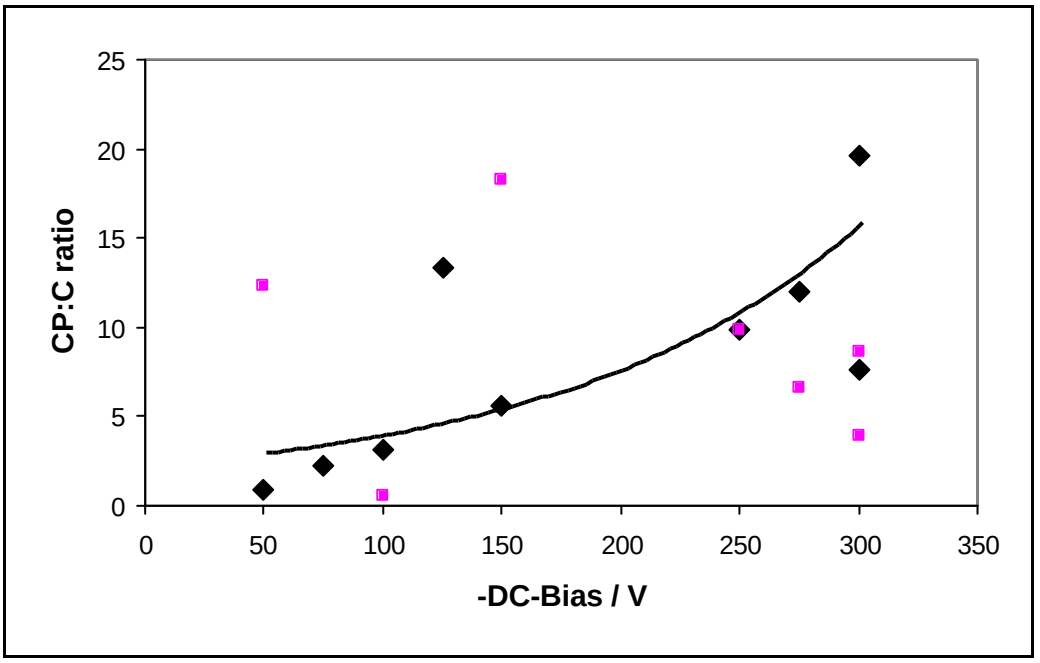

Figure 4.24: CP:C ratios for films measured from SIMS depth profiles plotted against deposition DC Bias. The black diamonds represent as-deposited films, the purple squares represent annealed films.

Figure 4.25 shows the optical band gap of several films plotted against the DC bias. It is observed that the optical band gap decreases with increasing DC bias. This is consistent with some theoretical predictions that fully sp^3-bonded crystalline carbon phosphide should have metallic character (*i.e.* zero band gap) and suggests that increasing the ion impact energy leads to a higher degree of sp^3 bonding in the films. Unfortunately as curve fitting in XPS is difficult with so many potential bonding environments this can only be hypothesised.

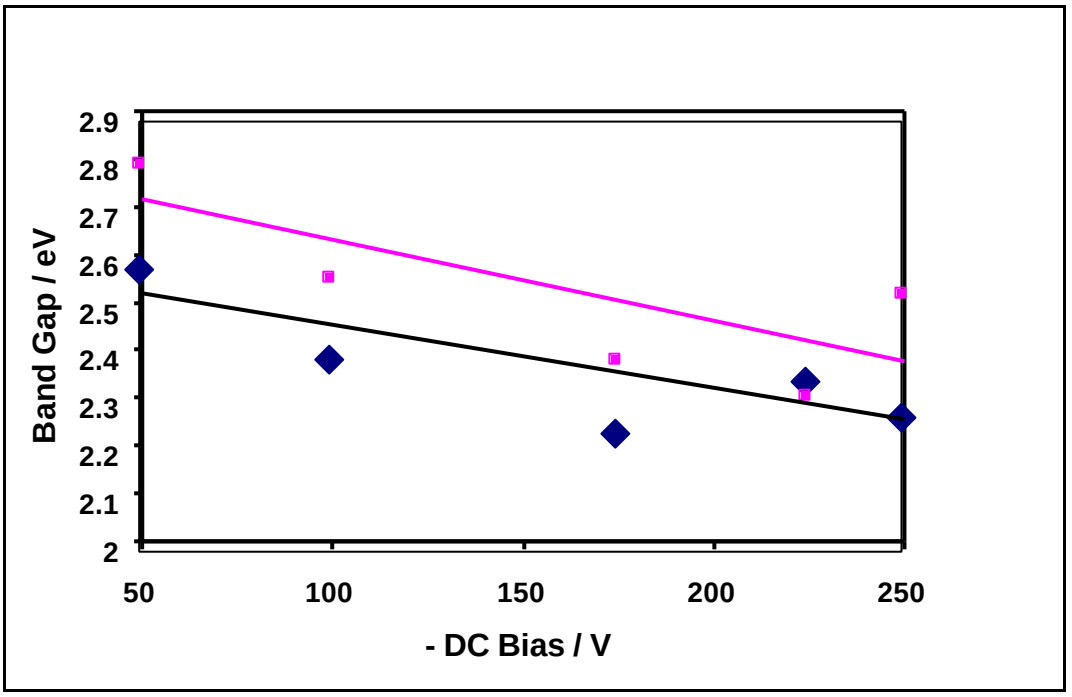

Figure 4.25: The optical band gap of several films measured by the Tauc plot method as a function of deposition DC bias. The black diamonds and black trend line represent as deposited films, the purple squares and trend line represent annealed films.

4.3.4 Annealed films

There was no significant difference on the appearance of annealed films to their as-deposited counterparts. Figure 4.22 shows the P:C ratio as measured by XPS against the DC-Bias voltage for films annealed at 300 ºC for 30 minutes. It can be

seen that there is a lot of scatter in the data, but the general trend is for the P:C ratio to decrease as in the as-deposited case. All of the films that were annealed had a lower P:C ratio than their as-deposited counterparts. This is thought to be due to non-bonded or loosely bonded P species being removed by the heating process. Figure 4.25 shows the estimation of optical band gap against the DC-Bias. It shows that as with the as-deposited film the optical band gap decreases with DC-Bias, but surprisingly the optical band gap seems to increase after annealing. This is the opposite of the results observed in annealed films deposited with different gas mixtures. In those results it was thought that the annealing may have been increasing the bonding between the carbon and phosphorus and maybe helped create an sp^3 type network, moving closer towards the structure of Claeyssens *et al*. The opposite is true here. Annealing these films is increasing the optical band gap, which shows that heating the films may be destabilising the sp^3 network in favour of an sp^2 or amorphous network. This has been seen in DLC, Annealing of DLC films at high temperatures has been shown to destabilise the sp^3 network[12].

Figure 4.23 and Figure 4.24 show the CP:P and the CP:C ratios measured by SIMS. It can be seen that the bonding between C and P generally increases upon annealing the films compared to as-deposited films, but there is a lot of scatter on the data. This may be due to sample handling issues (it was not always possible to wait for films to reach the base pressure of the annealing apparatus, which may introduce contaminants onto the film surface). This shows that annealing sometimes improves the C and P bonding. This may be due to the character of the films. At lower ion energies the films will be polymeric with lots of unbound C and P species. This is because the ion impact energy does not disturb the solid interface sufficiently to allow many strong

bonds to form. At higher energies this occurs. So annealing films that have been deposited at lower ion energies should either allow these bonds to form or allow these unbound species to leave the solid film. At higher ion energies many of these bonds will already exist and annealing these films may allow them to be broken again, as films deposited at various energies have such different properties, it is not surprising that they react differently when annealed. This explains the large scatter of the data.

4.3.5 XPS at the Synchrotron Radiation Light Source

The aim of this study was to reduce the linewidth of the XPS. A more detailed discussion of why this may reduce the linewidth is given in Chapter 3, but briefly, since the monochromated radiation from a synchrotron has both a thin line width and a high photon flux, it was hoped that it may allow the discrimination of individual peaks for certain types of bonding on the XPS (*e.g.* CP, CC, PP, CO *etc*). The samples made for this experiment were made especially for the study, but were made in identical conditions to the films used for the ion energy study and packed carefully in air tight vials under argon gas. Unfortunately there were problems both with the deposition and the analysis apparatus.

There was a leak in the phosphine MFC that unfortunately allowed air to mix with the phosphine gas. This was only a problem with the last few sets of films. Phosphine gas reacts violently with air, more specifically the oxygen in air. From the reaction with air it produces solid P_2O_5 and other phosphorus oxides. This clogged the shower head of the reactor and also caused the films to be highly oxidised.

In analysis the channeltron that detects the energy of photoelectrons was not working correctly. It suffered from ghosting and hence widened the spectra that came from it. Figure 4.26 shows C 1s and P 2p spectra from the XPS based in Bristol and the XPS based at the Synchrotron Radiation Light Source; from these it can be seen that the FWHM for the same type of film is wider in the case of the films analysed using synchrotron radiation. This was a great pity, as confidence was high that this may have given an absolute measure of the bonding between C and P in these films.

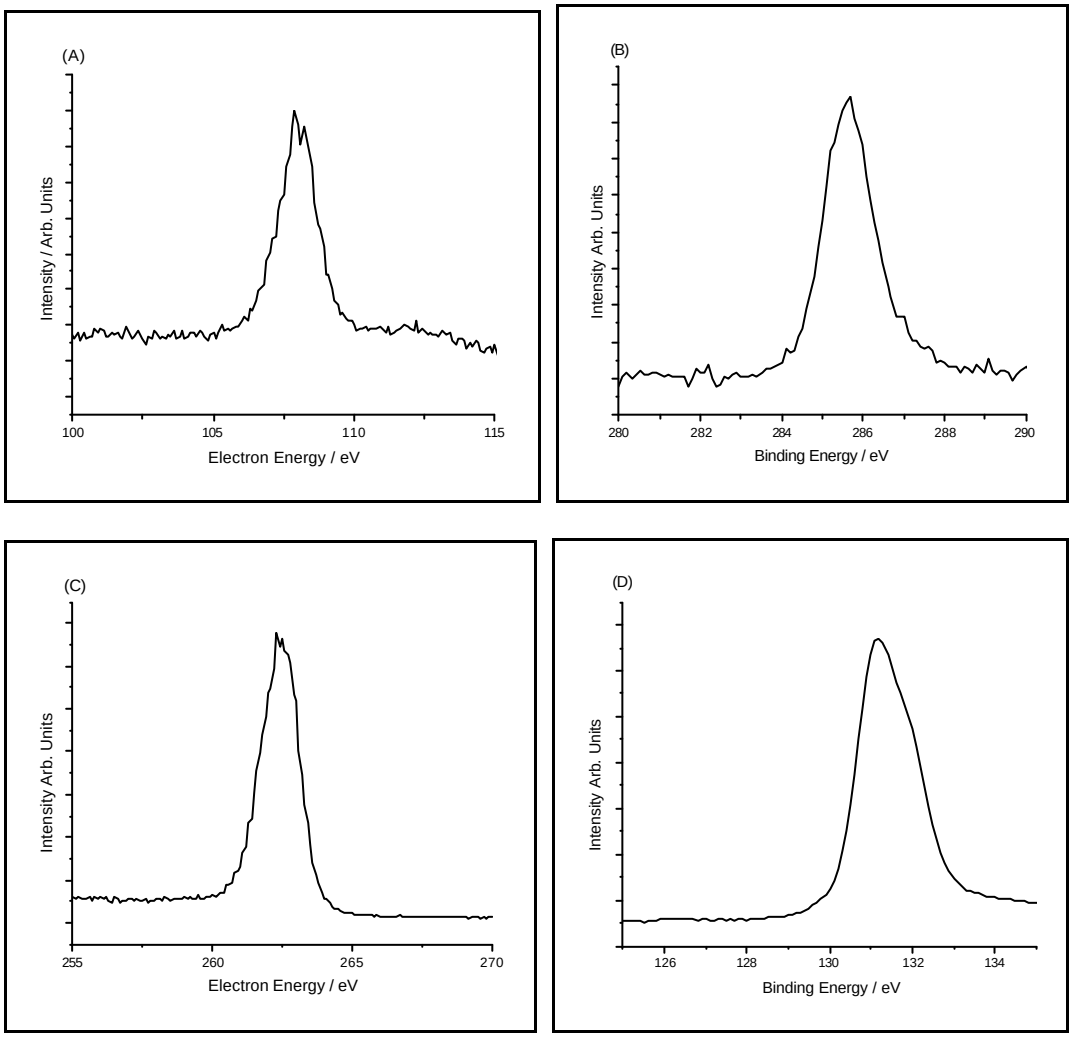

Figure 4.26: XPS Spectra taken at the facilities in the Interface Analysis Centre in Bristol and at the Synchrotron Radiation Light Source in Daresbury. (A) is a C 1s spectrum taken in Daresbury, (B) is a C 1s spectrum taken in Bristol, (C) is a P 2p spectrum taken in Daresbury and (D) is a P 2p spectrum taken in Bristol.

4.3.6 Conclusion

CP_x films have been grown that are virtually hydrogen free (below the ppm level detection limit of the SIMS) and virtually oxygen free. Increasing the DC bias and hence the ion impact energy during deposition has been shown both to increase the direct C-P bonding (by a mechanism involving preferential sputtering of non-bonded P species) and possibly to increase the degree of sp^3 bonding within the film leading to a reduction in optical band gap. Aspects of this study have been published in Diamond and Related Materials[23].

4.4 The effect of substrate temperature on the deposition of carbon phosphide thin films

4.4.1 Aims

In this section, results will be presented for film deposition at elevated substrate temperatures. The potential advantage of depositing onto a hot substrate is clear, in the above discussions post deposition heating of amorphous carbon phosphide thin films had a positive effect on the CP bonding and on the general stability of the film. It was hoped that an additional effect would be that the films would be crystalline. The rationale for this was that the *in situ* heating would give the film structure more energy during deposition and allow incoming species to bond in an organised manner. It would also allow non-bonded or incorrectly bonded species to bond correctly. The effect of deposition temperature on the CP bonding, the final chemical composition of the films and the optical band gap will be discussed.

4.4.2 Deposition and analysis parameters

All films were deposited using the RF-CVD chamber described in the experimental section. Films were deposited at DC-Biases between –150 and –250 V, with the same gas mixtures and pressures as in 4.3. The substrate was heated to between 50 and 300 ºC. As the heater power supply was removed before deposition, depositions were shortened to 10 minutes, in order to minimise heat loss during deposition. All films at each DC-Bias were grown in consecutive growth runs of decreasing temperature. This was due to the slow cooling of the substrate heater (the substrate heater took around 7 hours to cool from 250 ºC to room temperature), This also meant that films were removed from the reactor whilst still hot and this caused the films to be rapidly oxidised.

Three films were grown in each growth run. Two were grown on 100, B-doped Si and were used for simultaneous XPS and SIMS analysis. One was grown on quartz and was for UV/Vis analysis. The XPS used was the XPS at the Interface Analysis Centre. Film thicknesses were measured using focused ion beam etching and secondary electron imaging.

4.4.3 Results and discussion

Films deposited at high temperatures (>250 ºC) were transparent and colourless. SIMS depth profile analysis showed that this was because the film layer was extremely thin. Films deposited at lower substrate temperatures exhibited many colours from purple to red. Films deposited at a higher DC-Bias were coloured at a higher temperature indicating a greater film thickness. This is due to the higher

energy of incoming species bonding with the more energetic surface and subsurface compared to lower energy ions impacting onto the surface with a lower energy and not bonding as well. Figure 4.27 shows the growth rate of films at different substrate temperatures. It can be seen that the films deposited at higher DC-bias are indeed significantly thicker than those deposited at a lower DC-bias. There was no film detected at 300 ºC for the –150 V DC-bias. The growth rate also increased as the substrate temperature decreased. This is because the energy of the surface/subsurface will be lower at lower temperatures and will allow easier bonding with incoming species. For films deposited at room temperature it was found that the growth rate was much lower. It was thought that this may be due to the oxidation of films deposited at a higher substrate temperature, maybe with the absorption of moisture from the air. Films deposited at high temperatures were also harder than those deposited at low temperatures. Forceps did not scratch films deposited at temperatures higher than 150 ºC.

Figure 4.28 shows the P:C ratio measured by XPS for films deposited at various substrate temperatures. It can be seen that the P:C ratio stays more or less constant. From the XPS it was found that there was also a large amount of oxygen present in the films (for films deposited > 150 ºC the O content sometimes exceeded 50%). This was probably due to the removal of the films from the deposition apparatus whilst hot. It may also have been due to leaks within the gas metering system. SIMS depth profiles such as the one shown in Figure 4.29 show that although the surface oxygen content is high, it does not reduce below the surface to the low amounts that exist in films deposited in the other studies deposited at room temperature (for example in Figure 4.21). If the depth profile in Figure 4.29 is compared to that in Figure 4.21 it is

seen that even though the overall counts rate of O is higher in Figure 4.21, the number of counts compared to CP is lower. This is not the case in Figure 4.29 indicating that there may be an issue with the gas metering system or that the films allow oxygen to permeate through them at these higher temperatures.

Figure 4.29 also shows that the films are not of uniform composition throughout. This effect was seen in all films deposited in this study. It can be seen again that the H level is below the detection limit for SIMS throughout most of the film. Showing that the films are virtually H free.

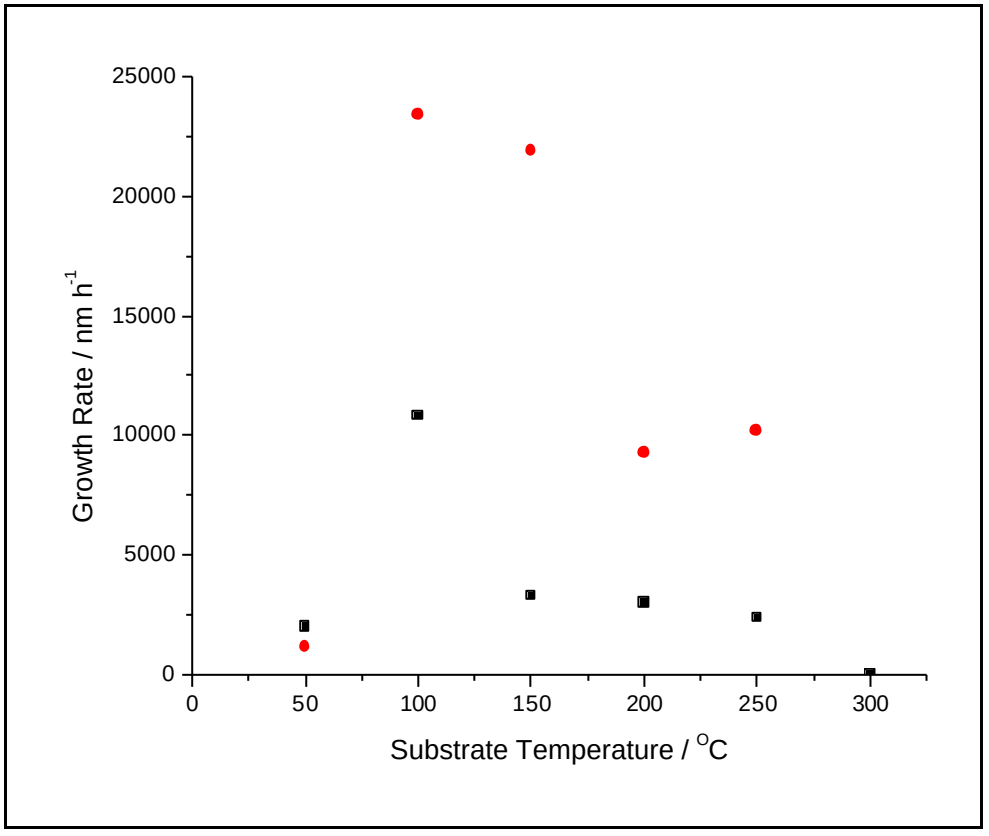

Figure 4.27: The growth rate of films deposited at different substrate temperatures. The black squares represent films that were deposited at –150 V DC-bias and the red circles represent films that were deposited at –250 V DC-bias

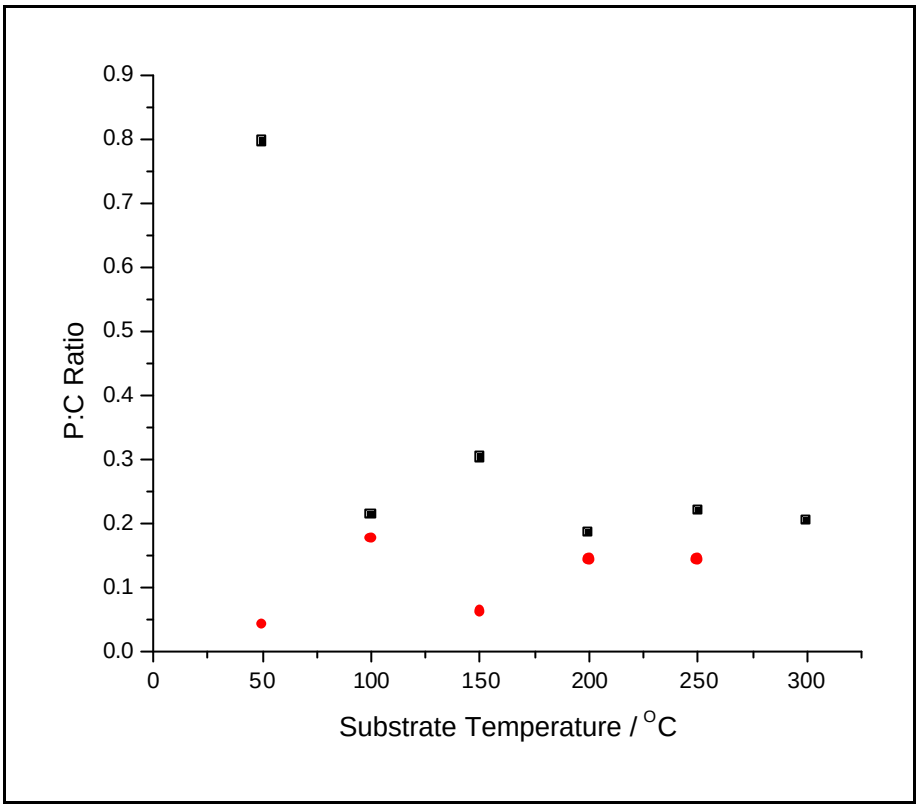

Figure 4.28: P:C ratio at the surface of films deposited at various substrate temperatures measured by XPS. The black squares represent films deposited at –150 V DC-bias and the red circles represent films deposited at –250 V DC-bias.

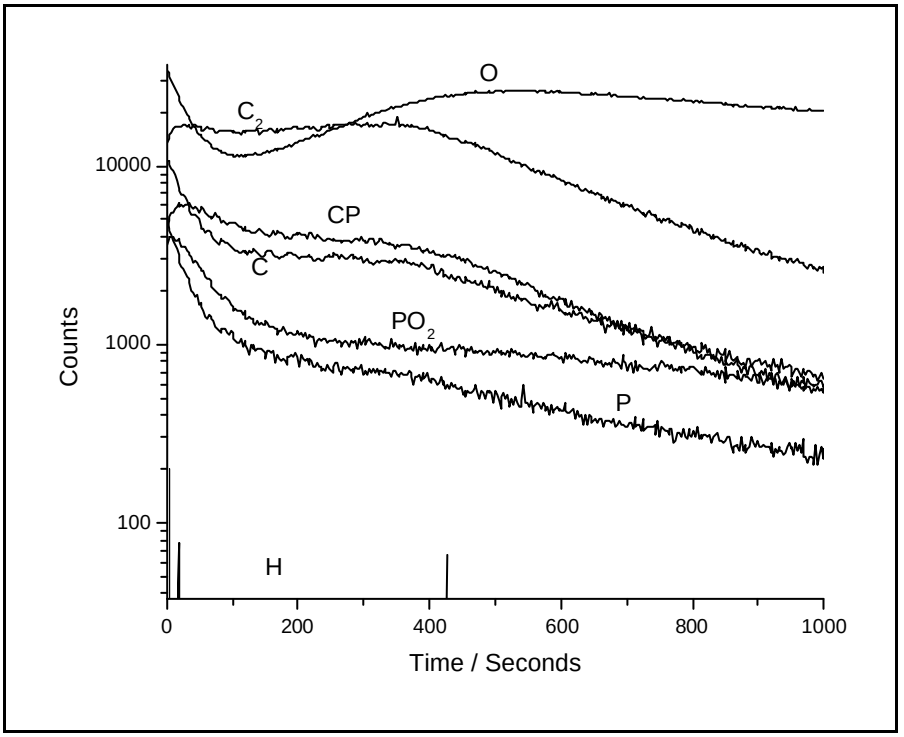

Figure 4.29: SIMS depth profile of a film grown at 200 ºC with a DC-bias of –150 V

Figure 4.30 shows the peak counts of CP:P and CP:C against substrate temperature, at two different DC-biases. It can be seen that the amount of CP compared with P and C decreases with increased substrate temperature. This is may be due to the low melting point of some types of phosphorus; the phosphorus may melt and aggregate. Also the films are highly oxidised, it is likely that the phosphorus is bonded to the oxygen as opposed to the carbon, for more oxidised films (the C-P bond enthalpy is 513.4 ±8 kJ mol^{-1} and the P-O bond enthalpy is 599.1 ±12.6 kJ mol^{-1} [21] so PO bonds are thermodynamically more favourable).

Figure 4.31 shows the optical band gap of thin films deposited at various temperatures. It can be seen that the optical band gap increases with the substrate temperature, and, as above, films deposited at higher ion energies have a lower optical band gap in general. This shows that there are some structural changes associated with the increase in substrate temperature. This may be due to the greater incorporation of O, or to the segregation of the components of the thin film.

This result is the opposite to that seen in DLC. A high substrate temperature at deposition in DLC increases the graphitic nature of the films[24,25] and hence usually decreases the optical band gap value.

X-ray powder crystallography of a number of these films found that they were not crystalline.

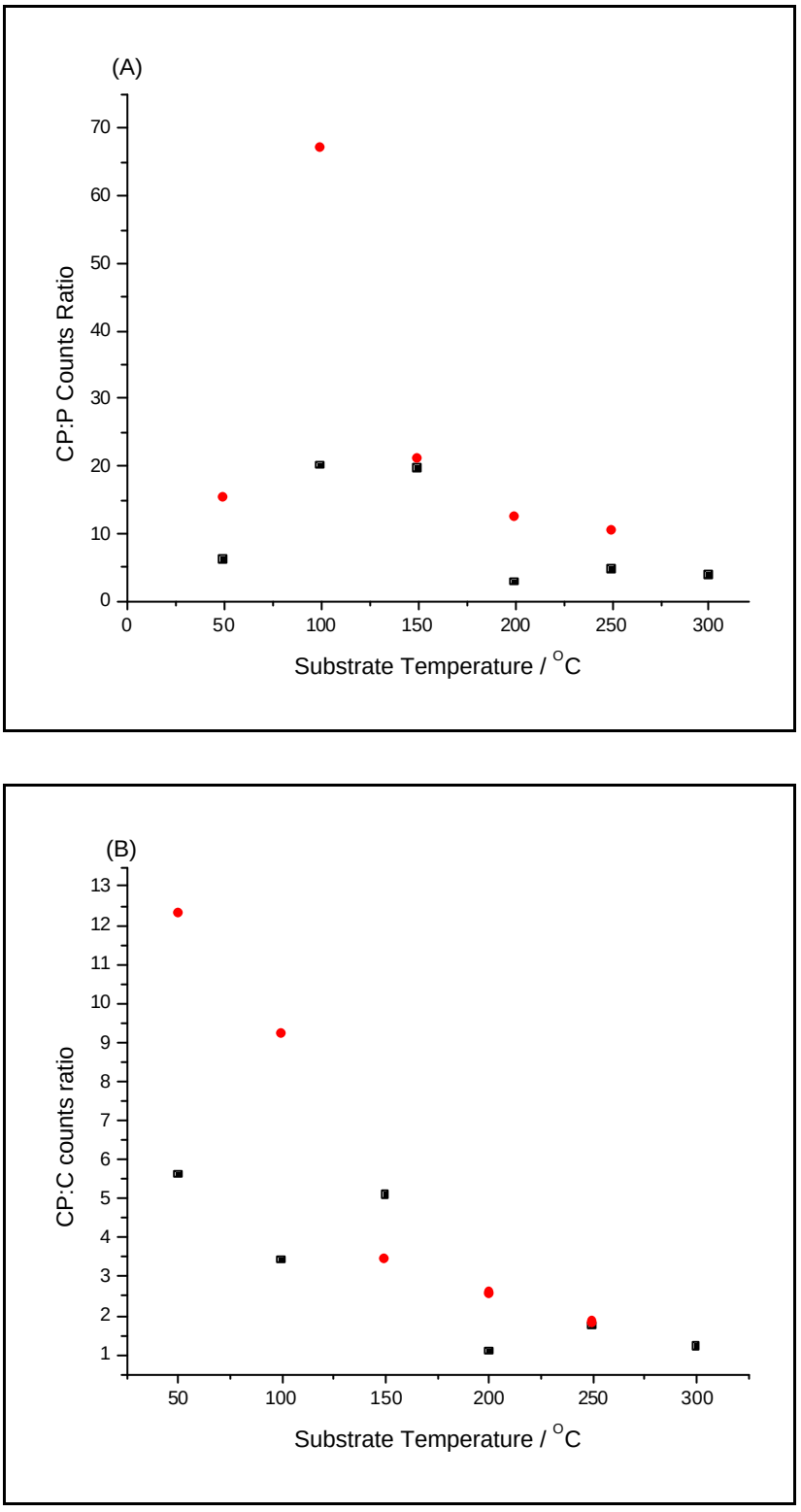

Figure 4.30: (A) CP:P counts ratios and (B) CP:C counts ratios for films deposited at varying substrate temperatures, the black squares represent films deposited at –150 V DC-bias and the red circles represent films deposited at –250 V DC-bias

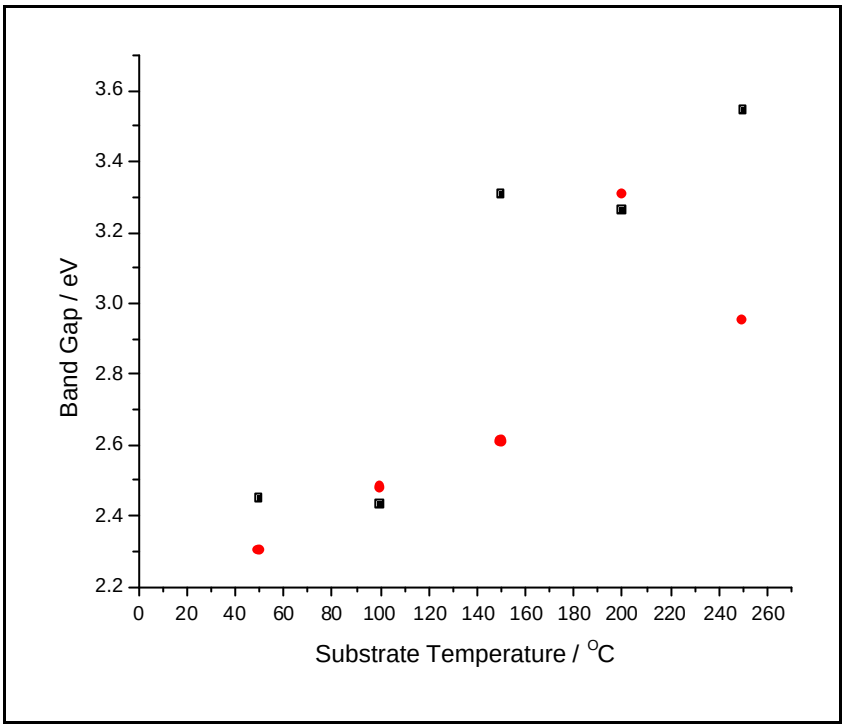

Figure 4.31: The optical band gap of films deposited at various substrate temperatures. The black squares represent films that have been deposited at a DC-bias of –150 V and the red circles represent films that have been deposited at –250 V.

4.4.4 Conclusions

Unfortunately due to the high amount of oxidation, higher substrate temperatures do not seem to increase the crystallinity of the films as hoped. Increasing the substrate temperature also seems to have a negative effect on the CP bonding. This may be due to the increased oxidation at high temperatures, but it may also be due to the phase separation of the P containing and C containing components of the film, especially with the low melting point of some types of phosphorus. The measurement of the CP bonding was done under the surface of the film and corresponded to the minimum amount of O counts in the film. Therefore the phase separation argument is more likely to be correct.

4.5 References

1 A. T. L. Lim, J. C. Zheng and Y. P. Feng, International Journal of Modern Physics B **16,** 1101-1104 (2002).

2 F. Claeyssens, N. L. Allan, P. W. May, P. Ordejon and J. M. Oliva, Chemical Communications**,** 2494-2495 (2002).

3 F. Claeyssens, J. M. Oliva, P. W. May and N. L. Allan, International Journal of Quantum Chemistry **In Press** (2003).

4 D. C. W. Shapton, BSc Thesis, University of Bristol, 1999.

5 T. Y. Leung, W. F. Man, P. K. Lim, W. C. Chan, F. Gaspari and S. Zukotynski, Journal of Non-Crystalline Solids **254,** 156-160 (1999).

6 P. Merel, M. Tabbal, M. Chaker, S. Moisa and J. Margot, Applied Surface Science **136,** 105-110 (1998).

7 *Handbook of X-ray Photoelectron Spectrscopy* (Perkin-Elmer Corp, 1992).

8 V. S. Veerasamy, G. A. J. Amaratunga, W. I. Milne, J. Robertson and P. J. Fallon, Journal of Non-Crystalline Solids **166,** 1111-1114 (1993).

9 M. Weiler, S. Sattel, K. Jung, H. Ehrhardt, V. S. Veerasamy and J. Robertson, Applied Physics Letters **64,** 2797-2799 (1994).

10 P. W. May, PhD Thesis, University of Bristol, 1991.

11 M. T. Kuo, PhD Thesis, University of Bristol, 2000.

12 J. Robertson, Materials Science & Engineering R-Reports **37,** 129-281 (2002).

13 J. Robertson, in *Amorphous Carbon: State Of The Art*, edited by S. R. P. Silva, J. Robertson, W. I. Milne and G. A. J. Amaratunga (World Scientific, 1997), p. 32-45.

14 J. Robertson, Diamond and Related Materials **3,** 361-368 (1994).

15 J. Filik, P. W. May, S. R. J. Pearce, R. K. Wild and K. R. Hallam, Diamond and Related Materials **12,** 974-978 (2003).

16 M. T. Kuo, P. W. May, A. Gunn, M. N. R. Ashfold and R. K. Wild, Diamond and Related Materials **9,** 1222-1227 (2000).

17 P. W. May, D. Field and D. F. Klemperer, Journal of Physics D-Applied Physics **26,** 598-606 (1993).

18 V. S. Veerasamy, G. A. J. Amaratunga, C. A. Davis, A. E. Timbs, W. I. Milne and D. R. McKenzie, Journal of Physics-Condensed Matter **5,** L169-L174 (1993).

19 D. Field, D. F. Klemperer, P. W. May and Y. P. Song, Journal of Applied Physics **70,** 82-92 (1991).

20 P. W. May, D. Field and D. F. Klemperer, Journal of Applied Physics **71,** 3721-3730 (1992).

21 *CRC Handbook of Chemistry and Physics*, 14 ed. (CRC Press, New York, USA, 1992).

22 S. R. J. Pearce, P. W. May, R. K. Wild, K. R. Hallam and P. J. Heard, Diamond and Related Materials **11,** 1041-1046 (2002).

23 S. R. J. Pearce, J. Filik, P. W. May, R. K. Wild, K. R. Hallam and P. J. Heard, Diamond and Related Materials **12,** 979-982 (2003).

24 B. K. Tay, X. Shi, E. Liu, H. S. Tan, L. K. Cheah, J. Shi, E. C. Lim and H. Y. Lee, Surface and Interface Analysis **28,** 226-230 (1999).

25 M. Tabbal, P. Merel, M. Chaker, M. A. El Khakani, E. G. Herbert, B. N. Lucas and M. E. O'Hern, Surface & Coatings Technology **119,** 452-455 (1999).